SPECIAL ISSUE: MOVING HEART FAILURE TO HEART SUCCESS: MECHANISMS, REGENERATION & THERAPY

Drug-based mobilisation of mesenchymal stem/stromal cells improves cardiac function post myocardial infarction

Veneta B. Todorova*, Nicoleta Baxan, Matthew Delahaye, Sian E. Harding and Sara M. Rankin

ABSTRACT

There is an unmet need for treatments that prevent the progressive cardiac dysfunction following myocardial infarction. Mesenchymal stem/stromal cells (MSCs) are under investigation for cardiac repair; however, culture expansion prior to transplantation is hindering their homing and reparative abilities. Pharmacological mobilisation could be an alternative to MSC transplantation. Here, we report that endogenous MSCs mobilise into the circulation at day 5 post myocardial infarction in male Lewis rats. This mobilisation can be significantly increased by using a combination of the FDA-approved drugs mirabegron (β_3-adrenoceptor agonist) and AMD3100 (CXCR4 antagonist). Blinded cardiac magnetic resonance imaging analysis showed the treated group to have increased left ventricular ejection fraction and decreased end systolic volume at 5 weeks post myocardial infarction. The mobilised group had a significant decrease in plasma IL-6 and TNF-α levels, a decrease in interstitial fibrosis, and an increase in the border zone blood vessel density. Conditioned medium from blood-derived MSCs supported angiogenesis in vitro, as shown by tube formation and wound healing assays. Our data suggest a novel pharmacological strategy that enhances myocardial infarction-induced MSC mobilisation and improves cardiac function after myocardial infarction.

KEY WORDS: MSCs, Mobilisation, Drug-based mobilisation, Cardiac repair, Mirabegron, AMD3100

INTRODUCTION

Mesenchymal stem/stromal cell (MSC) transplantation has been investigated in numerous pre-clinical and clinical trials as a method of tissue regeneration for a range of different diseases, including ischemic cardiomyopathy (Trounson and McDonald, 2015; Tompkins et al., 2018; Razeghian-Jahromi et al., 2021). Their therapeutic effects are thought to be mediated primarily by paracrine and trophic signalling, and include immunomodulation, extracellular matrix (ECM) remodelling, angiogenesis, cardiomyocyte protection, stimulation of cardiac progenitor cell proliferation and inhibition of fibrosis (Pittenger and Martin, 2004; Karantalis and Hare, 2015; Hatzistergos et al., 2010; Bagno et al., 2018; Guo et al., 2020). However, there are concerns in the field about the failure of clinical

trials to replicate the promising preclinical results (Galipeau and Sensébé, 2018). An explanation for this discrepancy may be the use of allogeneic cells in human trials, which are expanded to their replicative limit and cryopreserved prior to transplantation. This is in contrast to preclinical trials, where cells are usually syngeneic, harvested during their exponential growth phase and administered fresh (Galipeau and Sensébé, 2018). Importantly, extensive culture expansion can cause these cells to become senescent, which affects their gene expression, limits their homing abilities and interferes with their localisation to the site of injury (Honczarenko et al., 2006; Rombouts and Ploemacher, 2003).

To address these issues, we propose a novel approach of harnessing the therapeutic potential of endogenous MSCs, by increasing their mobilisation into the blood by using drugs. As a natural response to injury, such as skeletal trauma, skin burns, cardiomyopathies and acute myocardial infarction, stem/progenitor cells (including MSCs) mobilise into the circulation (Shintani et al., 2001; Wojakowski et al., 2004; Massa et al., 2005; Caplan and Correa, 2011; Girousse et al., 2021; Kucia et al., 2004). This is considered to be a part of the wound healing response, and we propose that, by increasing the extent of MSC mobilisation following injury through drugs, we can accelerate the resolution of inflammation and enhance tissue regeneration. Indeed, this strategy has already been validated in the context of skin wound and bone fracture healing (Hong and Son, 2014; Meeson et al., 2019). Such a drug-based regenerative approach would circumvent the cost and technical challenges associated with harvesting, culture expansion and transplantation of MSCs. Our goal here was to validate a pharmacological strategy to increase MSC mobilisation post myocardial infarction, and to test whether it can improve cardiac repair and function at the chronic stage (5 weeks) after myocardial infarction.

It is important to distinguish this work from previous research, which has investigated the use of granulocyte colony-stimulating factor (G-CSF) therapy for cardiac regeneration. Indeed, three double-blind placebo-controlled clinical trials showed that haematopoietic stem/progenitor cell (HSPC) mobilisation using G-CSF is ineffective at restoring the left ventricular ejection fraction (LVEF) (Zohlnhöfer, 2008; Engelmann et al., 2006; Ripa et al., 2005). These findings suggested that G-CSF treatment does not mobilise pro-reparative cell types, and it was later reasoned that MSCs would be a better cell type for regeneration (Ripa et al., 2006). We have previously reported that G-CSF alone or in combination with the CXCR4 antagonist AMD3100 does not mobilise MSCs, whereas the β3-AR agonist BRL37344 in combination with AMD3100 (Plerixafor) mobilises both MSCs and HSPCs (Pitchford et al., 2009; Fellous et al., 2020), thus having greater potential as a pro-reparative therapy. In support of this, in a model of bone healing we showed that the BRL37344+AMD3100 drug combination enhances tissue repair (Fellous et al., 2020).

Imperial College London, Faculty of Medicine, National Heart and Lung Institute, Myocardial Function, 72 Du Cane Road, London W12 0NN, UK.

*Author for correspondence (vt3017@ic.ac.uk)

V.B.T., 0000-0001-9762-3340; S.E.H., 0000-0002-3651-6354

Disease Models & Mechanisms

In this study, we chose to use the β3 adrenergic receptor (β3AR) agonist mirabegron as it has been approved by the United States Food and Drug Administration (FDA) and is thus more suitable for potential future translation into the clinic. Mirabegron has been approved for the treatment of overactive bladder disease and is also currently in a phase III clinical trial for heart failure (Warren et al., 2016; Pouleur et al., 2018). AMD3100 is FDA approved for use in combination with G-CSF for mobilisation of HSPCs to peripheral blood for collection and subsequent transplantation in patients with non-Hodgkin lymphoma or multiple myeloma (Wang et al., 2020), and was extensively studied in stem/progenitor cell mobilisation (Pitchford et al., 2009; Fellous et al., 2020; Redpath et al., 2017; Dar et al., 2011; Xu et al., 2011). Using a Lewis rat myocardial infarction model, we first identified the optimal time for pharmacological mobilisation by determining the peak day of myocardial infarction-induced MSC egress into the circulation. We then tested the ability the mirabegron and AMD3100, alone or in sequential combination, to enhance this myocardial infarction-induced mobilisation at day 5 post myocardial infarction and showed that only combination therapy, i.e. sequential treatment with mirabegron+AMD3100 (MA treatment) was successful. The effect of the MA treatment on cardiac function at 5 weeks post myocardial infarction was then evaluated.

RESULTS
Myocardial infarction mobilises endogenous stem/progenitor cells into the circulation
To assess the endogenous myocardial infarction-induced mobilisation of stem/progenitor cells into the blood, Lewis rats underwent either permanent ligation of the left anterior descending artery (LAD), leading to myocardial infarction or underwent control surgery (sham), whereby the suture was only passed through the tissue without tying

the LAD. Four paired groups (myocardial infarction and sham, n=4 each, total of 32 animals for the study) were terminated at different timepoints after myocardial infarction surgery, i.e. day 1, day 3, day 5 and day 10, and the numbers of circulating HSPCs and MSCs were assessed by quantifying colony-forming units (CFUs) and colony forming unit–fibroblasts (CFU-Fs), respectively. Circulating MSCs were significantly elevated on day 5 in the myocardial infarction group compared with those in the sham group (0.24 ± 0.47 (sham, n=4) vs 3.98 ± 3.78 (myocardial infarction, n=4) CFU-F/ml, P=0.0142) (Fig. 1A), whereas HSPCs were significantly elevated on day 1 (44.27 ± 30.4 (sham, n=4) vs 125.3 ± 32.52 (myocardial infarction, n=4) CFU/ml, P=0.043) (Fig. 1B). Furthermore, a lower level of bone marrow CFU-Fs was observed in the myocardial infarction group on day 1 compared to that in the sham group (Fig. 1C). There was no difference in the total circulating nucleated cells between sham and myocardial infarction at any timepoint (Fig. 1D). The plasma and bone marrow levels of chemokine CXCL12 were quantified by using sandwich enzyme-linked immunosorbent assay (ELISA). There was no difference in the concentration of CXCL12 in bone marrow aspirates of sham and myocardial infarction groups (Fig. 1F); however, in the myocardial infarction group, plasma levels of CXCL12 were significantly increased on day 5 after injury (Fig. 1E).

Combined sequential treatment with mirabegron+AMD3100 increased levels of circulating stem/progenitor cells after myocardial infarction
After establishing the peak day (day 5) of myocardial infarction-induced endogenous MSC mobilisation into the circulation, we investigated whether this can be further increased by application of mirabegron (daily gavage over 5 days) or AMD3100 (once at day 5) alone (M or A group, respectively) (Fig. S2B,C), or in combination
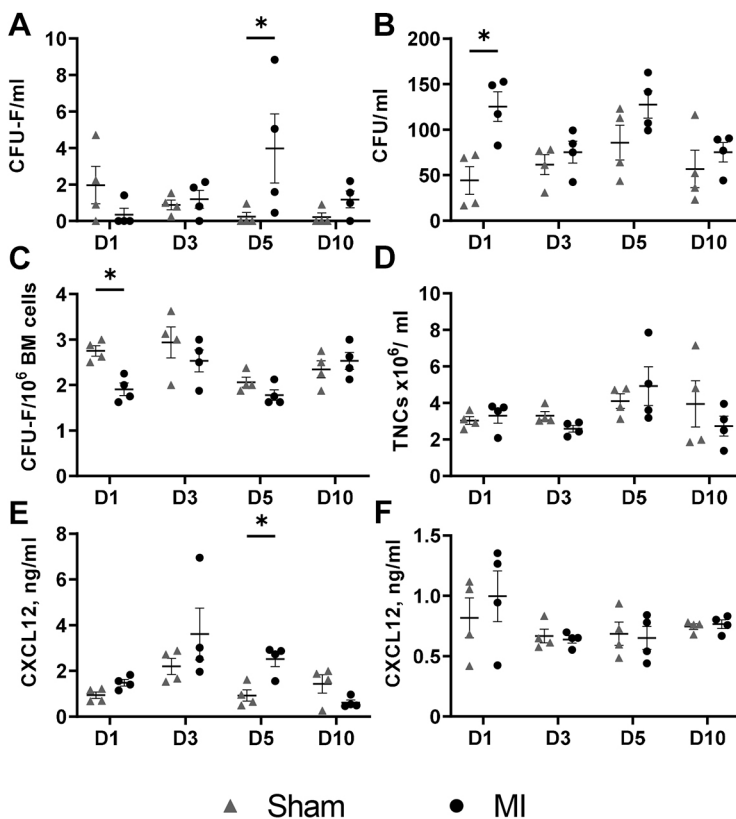

Fig. 1. Dynamics of stem/progenitor cell mobilisation after myocardial infarction. Male Lewis rats were sacrificed on day (D)1 to D10 after myocardial infarction (MI) (n=4 for each timepoint), or sham (n=4 for each timepoint) surgery, and their blood and bone marrow (BM) were collected for analysis. (A-C) To analyse endogenous myocardial infarction-induced mobilisation of stem/progenitor cells into the blood, we quantified the number of circulating MSCs (in CFU-F/ml) (A), circulating HSPCs (in CFU/ml) (B) and resident BM MSCs (in CFU-Fs per 1×10^6 seeded BM cells, i.e. in CFU-F/million) (C). (D) Circulating nucleated cells (TNCs) were measured in whole blood by using Turk's solution and are presented as total cells$\times10^6$/ml. (E,F) Levels of CXCL12 in the plasma (E) or BM (F) were measured (in ng/ml) using ELISA. Two-way repeated Measures ANOVA was performed on all datasets, Šidák's multiple comparisons test was performed on datasets A-C and E (*P<0.05).
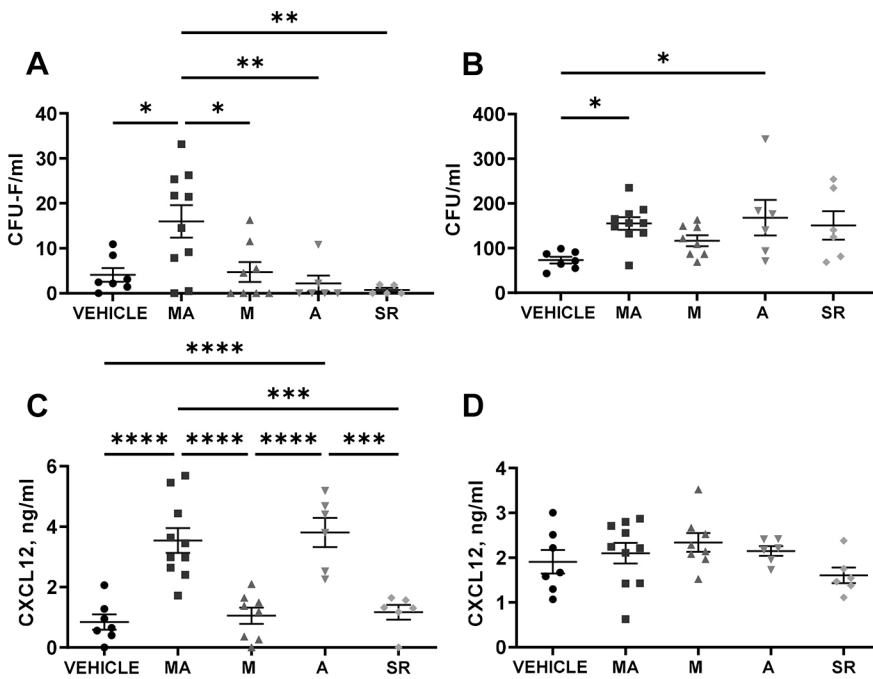
Fig. 2. Effect of drugs on stem/progenitor cell mobilisation after myocardial infarction. Five different treatment groups were assessed, i.e. rats after myocardial infarction surgery treated with vehicle (*n*=7), mirabegron followed by AMD3100 (MA; *n*=10), mirabegron only (M; *n*=8), AMD3100 only (A; *n*=6) or SR59230A only (SR; *n*=6). (A) Amounts of circulating MSCs were measured as CFU-F/ml. (B) Levels of circulating HSPCs were measured as CFU/ml. (C,D) Levels of CXCL12 in plasma (C) and bone marrow (D) were quantified using ELISA, and plotted in ng/ml. One-way ANOVA was performed on all datasets, Tukey's multiple comparisons test was performed on A-C, *$P<0.05$, **$P<0.01$, ***$P<0.001$, ****$P<0.0001$.

(MA group) (Fig. S2A). In addition, we tested whether treatment with the β₃AR antagonist SR59230A affects myocardial infarction-induced MSC mobilisation. For this, all animal groups underwent myocardial infarction surgery and, 24 h later, were given a daily dose of mirabegron (M), SR59230A (SR) or vehicle only for 5 days (Fig. S2C-E). The MA group was treated with mirabegron for 5 days, but, on the last day – 1 h after the last dose of mirabegron, animals also received a single dose of AMD3100 (Fig. S2A). The AMD3100 only (A) group received no pre-treatment but a single dose of AMD3100 on day 5 (Fig. S2B). Animals were sacrificed 1 h after the last drug had been administered. The results showed that mirabegron

(M) or AMD3100 (A) alone did not significantly increase circulating levels of CFU-Fs; however, sequential administration of both drugs (MA) caused an ∼4-fold increase compared to administration with vehicle (vehicle: 4.075±4.02, *n*=8 vs MA: 15.99±11.36 CFU-F/ml, *n*=10, *P*<0.05) (Fig. 2A). When using the same treatment protocols, these drugs did not induce MSC mobilisation in rats that had not undergone myocardial infarction surgery (MA, *n*=4, M, *n*=4, A, *n*=4, V, *n*=4). Both groups that had received AMD3100 showed elevated levels of circulating HSPCs and increased of CXCL12 plasma levels (Fig. 2B,C). No difference was seen in the bone marrow CXCL12 levels after any of the drug treatments (Fig. 3D). Whereas treatment
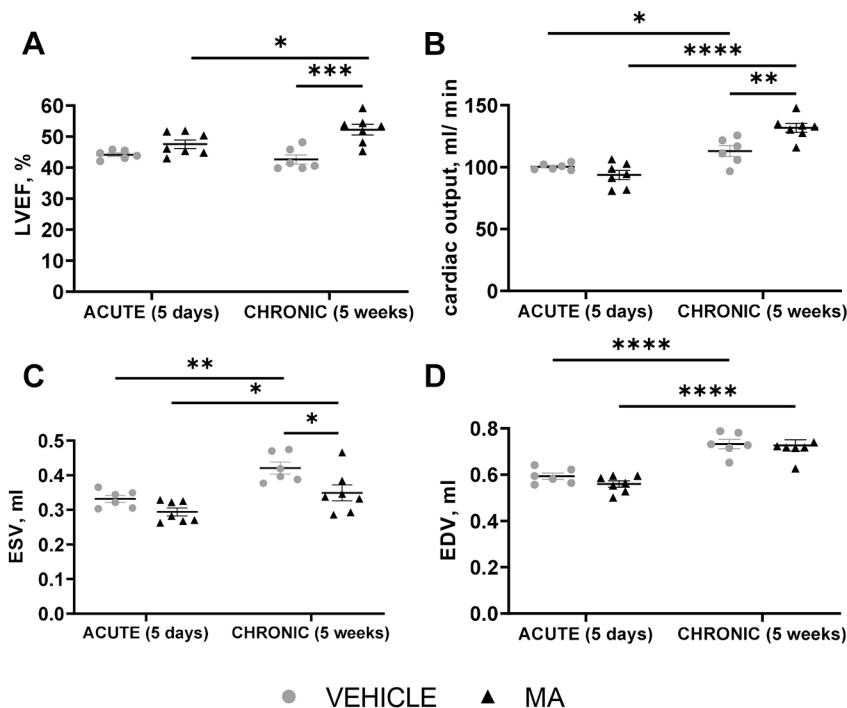

Fig. 3. MA-treated rats showed improved global cardiac contractility at 5 weeks post myocardial infarction compared to vehicle-treated rats. Male Lewis rats underwent myocardial infarction surgery followed by treatment with vehicle (*n*=6) or combined sequential treatment with mirabegron+AMD3100 (MA; *n*=7). (A-D) Cardiac function was validated by measuring left ventricular ejection fraction (LVEF) (in percentage) (A), cardiac output (in ml/min) (B), end-systolic volume (ESV) (in ml) (C) and end-diastolic volume (EDV) (in ml) (D) after treatment. Measurements were taken at day 5 and week 5 post myocardial infarction surgery, using blinded cardiac MRI. Two-way ANOVA was performed on all datasets, with Bonferroni post-tests on datasets A-C (*$P<0.05$, **$P<0.01$, ***$P<0.001$) and Šidák's multiple comparisons test on datasets A-D (*$P<0.05$, **$P<0.01$, ****$P<0.0001$).

with SR59230A led to the lowest levels of circulating CFU-Fs (Fig. 2A), no significant inhibition of myocardial infarction-induced MSC mobilisation was observed.

The cells that we here refer to as MSCs grew from the blood and bone marrow samples as CFU-Fs, and were plastic adherent with fibroblast-like appearance under a light microscope (Fig. S6A). Following their expansion in culture, they were analysed by using flow cytometry for their expression of MSC-like cell surface markers. The bone marrow-derived cells had a significantly larger CD45-positive population compared to their blood-derived counterparts [39.47±6.4%, bone marrow (*n*=6) vs 3.89±2.8%, blood (*n*=6), *P*=0.0022] (Fig. S6E). Culture-expanded bone marrow- and blood-derived CFU-Fs (>P5) were 96.8±0.28% and 97.82±1% positive for CD90 and CD29, respectively (gated on cells negative for CD45, CD31, CD43 and His48) (Fig. S6C,D), and successfully underwent chondrogenesis and osteogenesis; however, only the bone marrow-derived CFU-Fs from the vehicle and SR groups underwent adipogenesis (Fig. S6B).

MA treatment improved heart function at 5 weeks post myocardial infarction compared to treatment with vehicle

Data presented in Fig. 2 led us to next investigate whether MA treatment has an effect on cardiac function post myocardial infarction. To do this, we performed myocardial infarction surgery on Lewis rats and used blinded cardiac magnetic resonance imaging (MRI) analysis to investigate animals treated with vehicle (*n*=6) or MA (*n*=7) at day 5 (acute) and week 5 (chronic) after surgery. No changes in cardiac function were observed after treatment with vehicle or MA at day 5 post myocardial infarction (Fig. 3A-D). By contrast, at 5 weeks post myocardial infarction, the MA-treated group showed improved LVEF (vehicle: 42.61±3.53% vs treated: 51.99±4.43%, *P*<0.001) (Fig. 3A), cardiac output (vehicle: 112.96 ±10.7 ml/min vs treated: 132.03±9.58 ml/min, *P*<0.01) (Fig. 3B) and decreased end-systolic volume (ESV) (vehicle: 0.42±0.04 ml vs treated: 0.35±0.06 ml, *P*<0.05) (Fig. 3C). The end-diastolic volume (EDV) was increased between acute and chronic stages but not affected by MA treatment (Fig. 3D). Moreover, LVEF increased between day 5 and week 5 in the MA-treated but not the vehicle-treated group.

We then measured the size of the myocardial scar using two methods. Late gadolinium enhancement (LGE) was used *in vivo* at 5 days and 5 weeks; Masson's trichrome staining of heart sections was used *ex vivo* at 5 weeks post myocardial infarction. We did not observe differences in scar size between vehicle- and MA-treated groups at any timepoint (Fig. 4A,B). By using the Masson's trichrome-stained sections, we quantified the extent of interstitial fibrosis in the healthy region of the left ventricle and the border zone of the infarct. This analysis showed reduced interstitial fibrosis (collagen in %) in both healthy myocardium and the border zone of the infarct of the MA-treated group (Fig. 4C,D).

MA treatment increased blood vessel density in the border zone of the infarct

To determine whether MA treatment for MSC mobilisation affects blood vessel density, heart sections obtained from rats 5 weeks after myocardial infarction surgery were stained with the blood vessel marker isolectin-B4. Our blinded analysis showed that the MA-treated group had increased blood vessel density in the border zone of the infarct (Fig. 5B). No difference in blood vessel density within the scar tissue was seen between the groups (Fig. 5A).

Blood- and bone marrow-derived MSCs support angiogenesis *in vitro*

We next explored whether mobilised blood-derived MSCs secreted pro-angiogenic factors. To assess this, we compared the angiogenic potential of conditioned medium from blood- and bone marrow-derived MSCs *in vitro* by using human umbilical vein endothelial cell (HUVEC) tube formation and wound healing assays. The blood and bone marrow-derived MSCs used for these assays were culture expanded (>P5) after isolation from the MA and vehicle groups (day 5 post myocardial infarction). Conditioned medium was obtained by incubating the cells with serum-free DMEM for 24 h. Complete EGM-2 and serum-free DMEM served as positive and negative controls, respectively. Our results indicate that the conditioned medium from all MSCs significantly increased HUVEC tube formation compared to negative control (DMEM) (Fig. 6A-C). However, only the conditioned medium from the blood-derived MSCs from the MA group was significantly better than EGM-2 at supporting tube formation (Fig. 6A-C). Of note, conditioned medium from the blood-derived MSCs of the MA group had higher levels of secreted CXCL12 compared to its counterpart from bone marrow-derived MSCs (Fig. S8).

In the wound healing assay, all conditioned media mediated significantly more efficient wound closure compared to the DMEM negative control (Fig. 6D). However, whereas bone marrow MSC conditioned medium performed worse than EGM-2 positive control, blood MSC conditioned medium was no different, indicating that it is as good as the positive control at supporting wound closure (Fig. 6D).

MA treatment at 5 weeks post myocardial infarction decreases levels of IL-6 and TNF-α in plasma

Another known therapeutic effect of MSCs is immunomodulation. Thus, we investigated whether increasing numbers of circulating MSC at day 5 after myocardial infarction impacted the systemic inflammatory response. Analysis of plasma cytokine levels was performed using blood samples from the drug selection study with an endpoint at day 5, and the functional improvement study with an endpoint at week 5 post myocardial infarction. The data revealed that, at week 5 post myocardial infarction, MA treatment was associated with significant reductions in circulating levels of both IL-6 and TNF-α compared to levels after treatment with vehicle (Fig. 7A,B). Plasma levels of IL-10 did not differ between the groups at any timepoint but significantly increased over time in both groups (Fig. S9). Our data also show significant elevation of both IL-6 and TNF-α from day 5 to week 5 in the vehicle group, which was not observed in the MA-treated group (Fig. 7A,B). Although numbers of circulating MSCs and TNCs did not differ between the groups at 5 weeks post myocardial infarction, numbers of circulating HSPCs were significantly reduced in the MA group compared to that treated with vehicle (Fig. S10). These data suggest that MA treatment significantly reduces some aspects of the inflammatory response at 5 weeks post myocardial infarction.

DISCUSSION

Despite promising preclinical studies investigating culture-expanded MSC transplantation for cardiac repair, clinical trials using this approach have been largely disappointing (Galipeau and Sensébé, 2018). This may be due to technical and practical issues associated with culture expansion, handling and delivery of cell therapies. An alternative approach that circumvents these problems is to harness the regenerative potential of endogenously mobilised MSCs. In this study, we explored the use of drugs that enhance
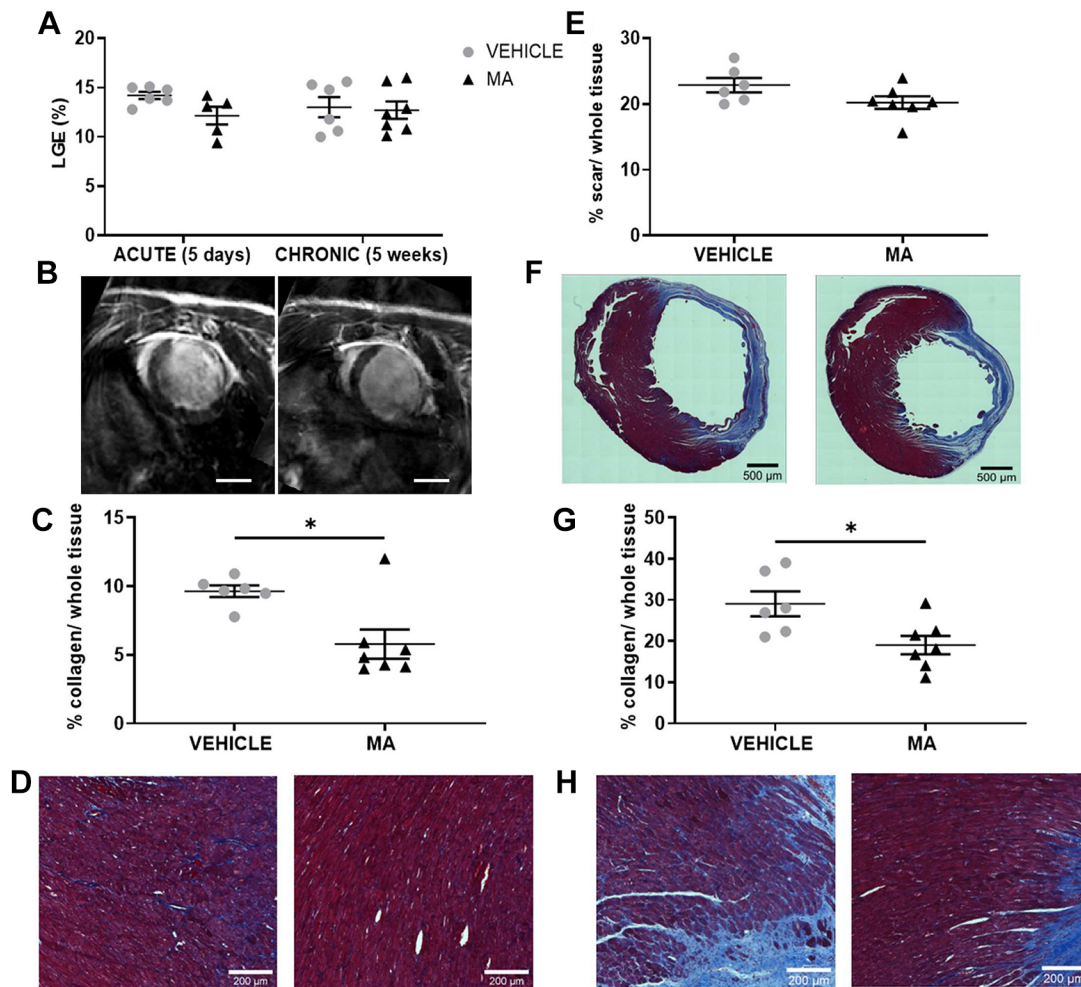
Fig. 4. Scar size and interstitial fibrosis. Male Lewis rats underwent myocardial infarction surgery followed by treatment with vehicle (grey circles; *n*=6) or combined sequential treatment with mirabegron+AMD3100 (MA; black triangles; *n*=7). (A,E) The size of the myocardial scar (in %) was assessed after 5 days and 5 weeks by using the late gadolinium enhancement (LGE) method *in vivo* (two-way ANOVA, vehicle *n*=6, MA, *n*=7) (A) or after 5 weeks only by using Masson's trichrome method *ex vivo* (unpaired Student's *t*-test, *P*=0.0935, vehicle *n*=6, MA, *n*=7) (E). (B) Representative images of rat hearts from the vehicle (left) or MA (right) groups analysed using LGE (images from the 5 weeks post myocardial infarction timepoint). Scale bars: 6 mm. (F) Representative images of Masson's trichrome-stained heart sections after treatment with vehicle (left) or MA (right); collagen is shown in blue, muscle tissue is shown in red. (C,G) Masson's trichrome-stained images were also used to quantify the interstitial fibrosis at 5 weeks post myocardial infarction as collagen (in %) over the whole tissue: healthy region of the left ventricle (Mann–Whitney test, *P*=0.0350) (C), border zone of the infarct (unpaired Student's *t*-test, *P*=0.0208, vehicle, *n*=6, MA *n*=7) (G). (D,H) Representative images of interstitial fibrosis in the healthy heart region after treatment with vehicle (left) or MA (right) (D), and in the border zone after treatment with vehicle (left) or MA (right) (H).

myocardial infarction-induced mobilisation of MSCs into the blood to promote cardiac tissue repair. Previous work from our group has identified a drug-based MSC mobilisation strategy (Pitchford et al., 2009; Redpath et al., 2017; Dar et al., 2011; Xu et al., 2011) that improved healing of orthopaedic injuries (Fellous et al., 2020). Here, we suggest that this regenerative pharmacology approach has potential for improving heart function post myocardial infarction.

In the first 24 h post myocardial infarction, there is an acute sterile inflammation response associated with the influx of inflammatory cells; this is followed by a resolution and repair response that commences 5-7 days post myocardial infarction, and leads to neovascularisation and scar formation (Prabhu and Frangogiannis, 2016). Our data show that, whereas myocardial infarction-induced mobilisation of HSPCs peaks at day 1, mobilisation of MSCs is delayed, peaking at day 5, coinciding with the transition to the resolution of inflammation (Ong et al., 2018). Compared to treatment with vehicle, the sequential treatment with the β3-AR agonist mirabegron and the CXCR4 antagonist AMD3100 (MA

treatment) led to significant increase in circulating MSCs at day 5 post myocardial infarction. MA treatment resulted in improved left ventricular function at 5 weeks post myocardial infarction, increased LVEF (vehicle vs treated: 42.61±3.53% vs: 51.99 ±4.43%, respectively; *P*<0.001) and reduced ESV. The LVEF results show a trend towards an almost normal LVEF, which in rat has been estimated to be ≥51.6% (Higuchi et al., 2007), and is close to the normal level of LVEF in humans (≥50%) (Ponikowski et al., 2016). The EDV was increased at week 5 (chronic stage) compared to day 5 (acute stage) in both treatment groups, which indicates the development of a heart failure phenotype. This was not attenuated by the MA drug combination, suggesting that our treatment did not prevent dilatation but improved systolic function. The increased contractility could, at least partly, be due to reduced levels of plasma IL-6 and TNF-α in the MA-treated group, decreased interstitial fibrosis and increased angiogenesis at the border zone of the infarct. It should be noted that we exclude the possibility of direct effects of the drug on cardiac function at the
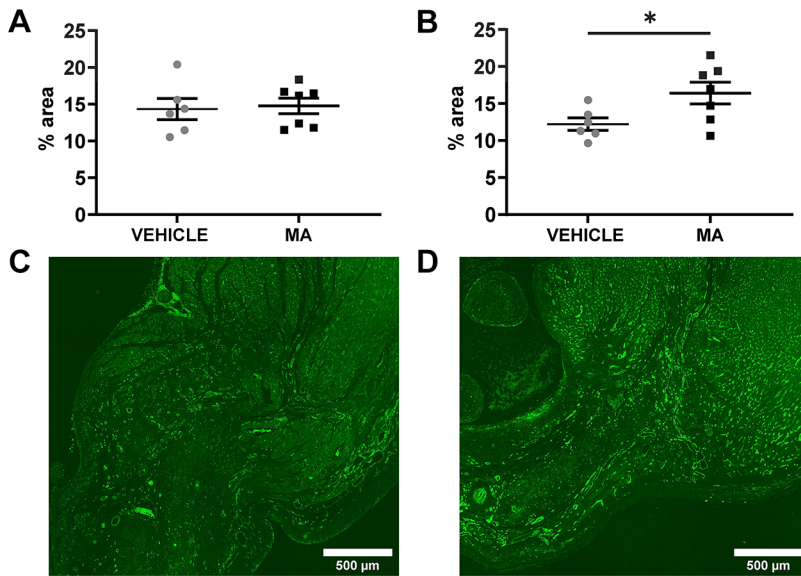
Fig. 5. Blood vessel density in the heart at 5 weeks post myocardial infarction. Blood vessel density was quantified by staining with isolectin-B4 in the heart tissue of vehicle-treated (grey circles; *n*=6) and MA-treated (black squares; *n*=7) rats 5 weeks after myocardial infarction surgery. (A,B) Plotted is the isolectin-B4-positive area (in %) for the scar zone (A) and the border zone (B) (unpaired Student's *t*-tests, *P*=0.8104 and *P*=0.0376, respectively). (C,D) Representative images of isolectin-B4-stained border zone after treatment with vehicle (C) or MA (D).

5-week timepoint because both drugs would have been completely cleared by then.

Previous studies have shown that IL-6 and TNF-α can both act as a cardiodepressant (Odeh, 1993; Pathan et al., 2011); thus, by lowering their levels we might have alleviated some of their cardiodepressive effects. Plasma levels of IL-6 increase with the severity of chronic heart failure and can – independently of LVEF levels – be prognostic for heart failure patients, showing the importance of this cytokine in the pathophysiology of the disease (Tsutamoto et al., 1998; Mann, 2015). IL-6 reduces the peak systolic Ca^{2+} transient and contractility by stimulating nitric oxide (NO) production, followed by a subsequent cyclic GMP-mediated dampening of L-type Ca^{2+} channel currents. IL-6 has also been shown to achieve sustained cardiodepression by directly triggering expression of inducible nitric oxide synthase (iNOS) in isolated cardiomyocytes (Finkel et al., 1992, 1993; Kinugawa et al., 1994). Similarly, it has been shown that TNF-α has a direct negative inotropic effect on contractile function in human, rat, hamster and
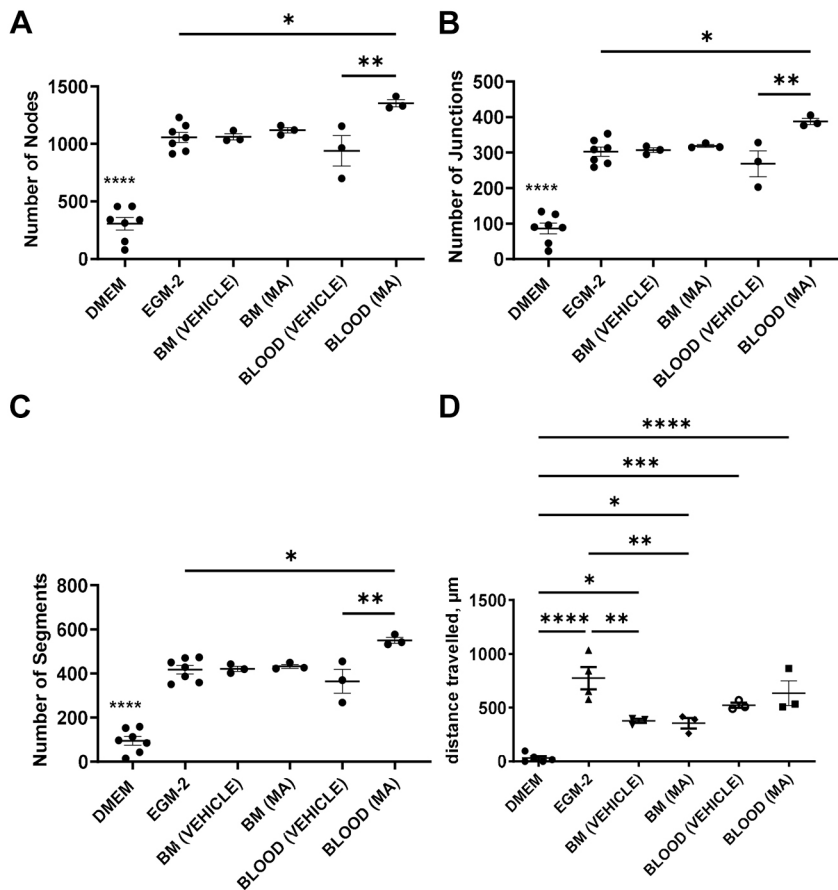

Fig. 6. *In vitro* HUVEC tube formation assay to assess the ability of blood and bone marrow MSC conditioned medium to support angiogenesis. Plotted are the effects conditioned media obtained from bone marrow- (BM) and blood-derived MSCs treated with vehicle or MA have on HUVEC tube formation. (A-D) Carried out were two *in vitro* angiogenesis assays, one assessing the ability of HUVECs to form a tube-like structure – quantified by the number of nodes (A), junctions (B) and segments (C) – and one assessing HUVEC migration in the context of wound healing (closing a manually introduced gap by scratching the plate) (D), quantified as distance travelled (μm) during 24 h. DMEM was used as negative control, EGM-2 as positive control. One-way ANOVA, Tukey's multiple comparisons test, **P*<0.05, ***P*<0.01, ****P*<0.001, *****P*<0.0001, *n*=3.
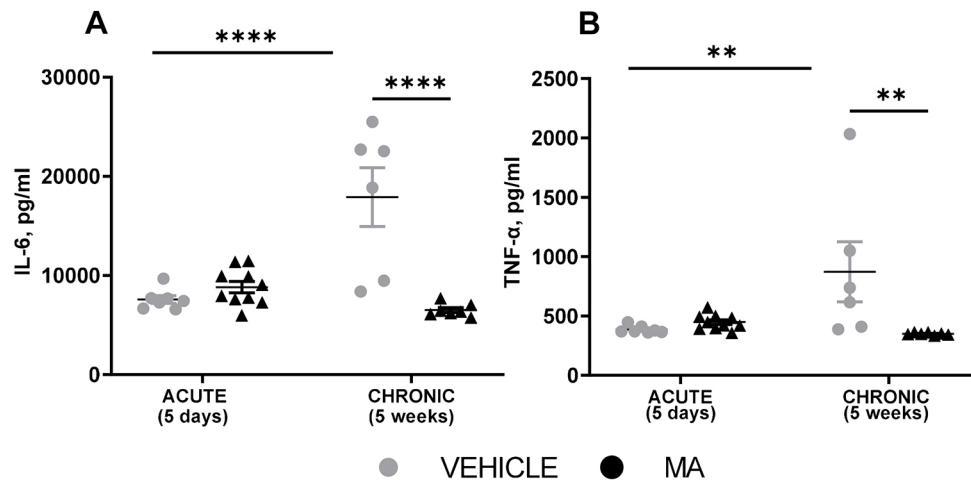
Fig. 7. Circulating cytokines on day 5 and week 5 post myocardial infarction. Male Lewis rats underwent myocardial infarction surgery followed by treatment with vehicle (grey circles) or combined sequential treatment with mirabegron+AMD3100 (MA; black triangles) after 5 days (acute) or 5 weeks (chronic). Sandwich ELISA was performed on plasma samples from vehicle- and MA-treated groups to determine whether MA treatment affects the levels of the pro-inflammatory cytokines IL-6 and TNF-α. (A,B) Plotted are levels of IL-6 (A) and TNF-α (B) on day 5 (vehicle $n=7$, MA, $n=10$) and week 5 (vehicle $n=6$, MA, $n=7$) post myocardial infarction. Results are shown in pg/ml. All datasets were analysed using two-way ANOVA and Šidák's post-tests, **$P<0.01$, ****$P<0.0001$.

dog myocardium (Finkel et al., 1992; Cain et al., 1998, 1999; Rathi et al., 2002; Thielmann et al., 2002). This appears to be mediated through altered Ca^{2+} handling, manifested by impaired Ca^{2+}-induced Ca^{2+} release and reduced myofilament sensitivity to Ca^{2+} (Saini et al., 2005). Finally, it must be noted that efficient early inflammation is required for transitioning to the resolution phase, which could explain the conflicting results in the literature showing pro-inflammatory cytokines as both needed for and deleterious to cardiac repair and regeneration (Prabhu and Frangogiannis, 2016).

A decrease in interstitial fibrosis was also observed in the MA-treated group. Interstitial fibrosis usually leads to increased myocardial stiffness and diastolic dysfunction (Zile et al., 2015). Moreover, excessive collagen deposition might negatively impact systolic function of the left ventricle by hindering cardiomyocyte force transmission and perfusion, impairing excitation-contraction coupling, disrupting the link between ECM and the sarcomeric contractile apparatus, and activating interstitial cells that secrete factors suppressing cardiomyocyte function (Frangogiannis, 2019; Iwanaga et al., 2002). Thus, decreasing interstitial fibrosis could be one of the mechanisms behind the improved systolic function of the left ventricle we observed at 5 weeks post myocardial infarction in the MA-treated group.

Stimulation of angiogenesis is one of the main mechanisms of MSC-mediated tissue regeneration (Gomez-Salazar et al., 2020), and is mainly mediated by secretion of proangiogenic factors, such as fibroblast growth factor (FGF), vascular endothelial growth factor (VEGF), platelet-derived growth factor (PDGF), angiopoietin, and others. Many such factors are upregulated with hypoxia, indicating a possibility of increased expression upon reaching the ischemic site of injury (Kinnaird et al., 2004). Here, we showed that the MA-treated group had increased blood vessel density in the border zone of the infarct. Moreover, by using HUVEC tube formation and wound healing assays, we showed the ability of blood-derived MSCs to support angiogenesis *in vitro*. This observation was not only in support of our *in vivo* results but also provided new evidence that blood-derived MSCs support angiogenesis *in vitro*, a finding that, so far, has mainly been reported for *ex vivo* expanded

tissue-resident cells, such as bone marrow- and adipose tissue-derived MSCs (Maacha et al., 2020).

Our data propose several insights into the molecular mechanisms that regulate myocardial infarction-induced MSC mobilisation and its pharmacological enhancement. The CXCR4 antagonist AMD3100 has the unique ability to reverse the gradient of CXCL12 across the bone marrow endothelium, causing an acute increase in plasma levels of CXCL12. This phenomenon was shown to be crucial for HSPC and MSC mobilisation from the bone marrow (Fellous et al., 2020; Redpath et al., 2017; Dar et al., 2011) and, recently, the molecular pharmacology underlying this response has been elucidated (Jørgensen et al., 2021). Our previous work has shown that the pharmacological mobilisation of MSCs is a two-step process, with the first step involving β_3AR agonism in the bone marrow, leading to increased local production of endocannabinoids and N-acyl ethanolamines, whereas the second step – driven by acute administration of AMD3100 – required the aforementioned reversal of the CXCL12 gradient across the bone marrow endothelium (Fellous et al., 2020). In line with this observation, we showed in this study that myocardial infarction-induced mobilisation of endogenous MSCs at day 5 post injury coincided with a significant increase of plasma CXCL12, suggesting involvement of this chemokine in the physiological mobilisation process. The plasma CXCL12 levels were further elevated after AMD3100 treatment, in both the MA and A groups. Moreover, the MA and A groups also had elevated circulating HSPC levels compared to vehicle, but only the MA group had elevated circulating MSC levels, consistent with our previous work showing that pre-treatment with mirabegron is necessary for MSC mobilisation (Fellous et al., 2020). Finally, we recorded the lowest levels of circulating MSCs in the β3-AR antagonist (SR59230A)-treated group, although no significant inhibition of myocardial infarction-induced MSC mobilisation was present. This observation warrants further research. However, we showed here that both CXCL12 and β3-AR signalling are needed, and neither is sufficient for the pharmacological enhancement of myocardial infarction-induced MSC mobilisation, as mirabegron only or AMD3100 only did not result in significant increase of circulating MSCs.

MSCs were identified by their CFU-F-forming ability, morphology, cell surface marker expression and ability to undergo trilineage differentiation. It is noteworthy that the circulating MSCs exhibit all these characteristics, except for differentiation into adipocytes. This suggests that circulating MSCs are osteochondral progenitors or another distinct subset of MSC progenitors. Future work will be required to more thoroughly investigate the similarities and differences between tissue-resident and circulating MSCs by using RNA-seq or other 'omics' approaches.

A limitation of our study is the lack of definitive evidence that mobilised MSCs are, indeed, trafficking to the site of the myocardial injury. Owing to the lack of a specific marker for rat MSCs and the limited understanding of their *in vivo* identity, it is currently impossible to track these cells *in vivo*. Nevertheless, the functional effects we have observed are consistent with the known functions of MSCs.

In conclusion, we have shown that endogenous stem/progenitor cells (MSCs and HSPCs) mobilise into the blood with distinct kinetics in response to myocardial infarction. We demonstrated that this myocardial infarction-induced MSC mobilisation can be enhanced at day 5 post myocardial infarction using a combination of two drugs approved by the FDA, i.e. mirabegron and AMD3100 (MA). The group receiving this treatment had improved cardiac contractility at 5 weeks post myocardial infarction and enhanced blood vessel density in the border zone of the infarct, decreased interstitial fibrosis, and reduced levels of the plasma pro-inflammatory cytokines (IL-6 and TNF-α). Based on this report, we suggest a novel, non-invasive, cost-efficient and easily translatable regenerative pharmacological approach for improving cardiac function after myocardial infarction.

MATERIALS AND METHODS
Animal care and procedures
Male Lewis rats (*rattus norvegicus*) purchased from Charles River Laboratories were used for all experiments. Rats weighed between 250 and 300 g. To create the rat myocardial infarction model permanent ligation of the left anterior descending artery (LAD) surgery was performed as described before (Prabhu and Frangogiannis, 2016). For this, animals were anaesthetised using 5% isoflurane and anaesthesia was maintained using 2-3% isoflurane. For local anaesthesia around the site of the initial incision, four injections of 10 μl bupivacaine hydrochloride and epinephrine (Marcaine 0.5%) were administered. Following surgery, carprofen (5 mg/kg/day) and buprenorphine (0.05 mg/kg/day) were administered subcutaneously for pain control during the first 2 days after surgery. Animal housing and treatment was done in accordance with the Animals (Scientific Procedures) Act 1986 Amendment Regulations 2012, and European Union directive 2010/63/EU.

To study post myocardial infarction progenitor mobilisation, we evaluated four timepoints, i.e. day 1, 3, 5 and 10, after myocardial infarction (*n*=4 for each timepoint) (Fig. S1). At each timepoint, a terminal procedure to collect bone marrow and peripheral blood was performed. The samples were used for quantification of stem/progenitor cells and total nucleated cell frequency, and CXCL12 levels. For the drug selection study, all rats underwent myocardial infarction surgery and were assigned to one of five treatment groups, i.e. vehicle (*n*=7), mirabegron only (M) (*n*=8), AMD3100 only (A) (*n*=6), mirabegron+AMD3100 (MA) (*n*=10) or SR59230A (SR) (*n*=6). Rats were then given the corresponding drugs and, on day 5, bone marrow and peripheral blood were collected for analysis (Fig. S2). The plasma from these animals was used for the day 5 timepoint for cytokine and chemokine assessment. The final animal study was the long-term evaluation of the effect of mirabegron+AMD3100 (MA) (*n*=7) on cardiac function compared to vehicle (*n*=6) (Fig. S3), which assessed cardiac function by using blinded cardiac MRI analysis at two timepoints post myocardial infarction, i.e. day 5 (acute) and 5 weeks (chronic). Animals

were sacrificed after performing the chronic timepoint MRI, and blood and bone marrow were collected for analysis.

Cell culture, quantification and characterisation of stem/progenitor cells
To isolate the mononuclear cells from the blood, the Ficoll-Paque density gradient centrifugation method was used as per manufacturer's instructions. Bone marrow cells were isolated from femurs and the red blood cells (RBCs) were lysed using the RBC lysing solution (eBioscience). For the CFU-F assay, blood mononuclear or bone marrow cells were plated at $0.32 \times 10^6/cm^2$ in Dulbecco's modified Eagle's medium (DMEM), supplemented with 20% foetal bovine serum (FBS), and cultured for 7 days prior to the first change of medium. Thereafter, medium was changed 2-3 times a week. Fibroblast-like colonies were manually counted under a light microscope on day 14, after seeding in a blinded fashion. Colonies were expanded in culture for flow cytometry and differentiation analysis (Table S1, Figs S4, S5 and S7). For quantification of HSPCs, MethoCult™ GF R3774 medium was used as per the manufacturer's instructions (StemCell). CFUs were manually counted on day 10 post seeding in a blinded fashion.

Quantification of CXCL12, IL-6, TNF-α and IL-10
Protein concentrations of chemokine CXCL12 and cytokines IL-6, TNF-α and IL-10 were analysed using the sandwich ELISA method (see Supplementary Materials and Methods).

Quantification of blood vessel density and interstitial fibrosis
Details about preparation of heart tissue for histology are included in the Supplementary Materials and Methods, together with the methods for the quantification of blood vessel density using isolectin-B4 and interstitial fibrosis using Masson's trichrome stained heart sections (see Supplementary Materials and Methods).

In vitro angiogenesis assays
HUVECs were purchased from Lonza and used between passages 1 and 6. For tube formation assays, we used the Ibidi μ-Slide Angiogenesis slides as per the manufacturer's instructions. Example images of tube formation assays are shown in Fig. S11. Wound healing assays were performed as described previously (Ong et al., 2018), and example images are shown in Fig. S11B. Detailed protocols can be found in the Supplementary Materials and Methods. Images were taken on a widefield microscope (AxioObserver Z1) and analysed using ImageJ. For tube formation assays, we used an Angiogenesis Analyser macro developed for ImageJ (Higuchi et al., 2007).

Cardiac MRI
Cine MRI was used to assess global heart function and LGE for quantifying myocardial scar size on day 5 and week 5 post myocardial infarction (see Supplementary Materials and Methods). Data analysis was performed by two independent users in a blinded fashion, using a semi-automated left ventricle segmentation software in the freely available program Segment (Ponikowski et al., 2016; Odeh, 1993).

Statistical analysis
For statistical analysis (Student's *t*-tests, one-way ANOVA, two-way ANOVA, normality tests, etc.), we used GraphPad 9.1 software. For all comparisons, $P<0.05$ was considered significant. Data are presented as the mean±standard error of the mean (s.e.m.).

for his help with imaging and image analysis. We also acknowledge the support of the Central Biomedical Services (CBS) at Imperial College London.

References
Bagno, L., Hatzistergos, K. E., Balkan, W. and Hare, J. M. (2018). Mesenchymal stem cell-based therapy for cardiovascular disease: progress and challenges. *Mol. Ther.* **26**, 1610-1623. doi:10.1016/j.ymthe.2018.05.009

Cain, B. S., Meldrum, D. R., Dinarello, C. A., Meng, X., Banerjee, A. and Harken, A. H. (1998). Adenosine reduces cardiac TNF-α production and human myocardial injury following ischemia-reperfusion. *J. Surg. Res.* **76**, 117-123. doi:10.1006/jsre.1998.5304

Cain, B. S., Meldrum, D. R., Meng, X., Dinarello, C. A., Shames, B. D., Banerjee, A. and Harken, A. H. (1999). p38 MAPK inhibition decreases TNF-α production and enhances postischemic human myocardial function. *J. Surg. Res.* **83**, 7-12. doi:10.1006/jsre.1998.5548

Caplan, A. I. and Correa, D. (2011). The MSC: an injury drugstore. *Cell Stem Cell* **9**, 11-15. doi:10.1016/j.stem.2011.06.008

Dar, A., Schajnovitz, A., Lapid, K., Kalinkovich, A., Itkin, T., Ludin, A., Kao, W.-M., Battista, M., Tesio, M., Kollet, O. et al. (2011). Rapid mobilisation of hematopoietic progenitors by AMD3100 and catecholamines is mediated by CXCR4-dependent SDF-1 release from bone marrow stromal cells. *Leukemia* **25**, 1286-1296. doi:10.1038/leu.2011.62

Engelmann, M. G., Theiss, H. D., Hennig-Theiss, C., Huber, A., Wintersperger, B. J., Werle-Ruedinger, A.-E., Schoenberg, S. O., Steinbeck, G. and Franz, W.-M. (2006). Autologous bone marrow stem cell mobilisation induced by granulocyte colony-stimulating factor after subacute ST-segment elevation myocardial infarction undergoing late revascularization. *J. Am. Coll. Cardiol.* **48**, 1712-1721. doi:10.1016/j.jacc.2006.07.044

Fellous, T. G., Redpath, A. N., Fleischer, M. M., Gandhi, S., Hartner, S. E., Newton, M. D., François, M., Wong, S.-P., Gowers, K. H. C., Fahs, A. M. et al. (2020). Pharmacological tools to mobilise mesenchymal stromal cells into the blood promote bone formation after surgery. *NPJ Regener. Med.* **5**, 3. doi:10.1038/s41536-020-0088-1

Finkel, M. S., Oddis, C. V., Jacob, T. D., Watkins, S. C., Hattler, B. G. and Simmons, R. L. (1992). Negative inotropic effects of cytokines on the heart mediated by nitric oxide. *Science* **257**, 387-389. doi:10.1126/science.1631560

Finkel, M. S., Hoffman, R. A., Shen, L., Oddis, C. V., Simmons, R. L. and Hattler, B. G. (1993). Interleukin-6 (IL-6) as a mediator of stunned myocardium. *Am. J. Cardiol.* **71**, 1231-1232. doi:10.1016/0002-9149(93)90654-U

Frangogiannis, N. G. (2019). Cardiac fibrosis: cell biological mechanisms, molecular pathways and therapeutic opportunities. *Mol. Asp. Med.* **65**, 70-99. doi:10.1016/j.mam.2018.07.001

Galipeau, J. and Sensébé, L. (2018). Mesenchymal stromal cells: clinical challenges and therapeutic opportunities. *Cell Stem Cell* **22**, 824-833. doi:10.1016/j.stem.2018.05.004

Girousse, A., Mathieu, M., Sastourné-Arrey, Q., Monferran, S., Casteilla, L. and Sengenès, C. (2021). Endogenous mobilisation of mesenchymal stromal cells: a pathway for interorgan communication? *Front. Cell Dev. Biol.* **8**, 598520. doi:10.3389/fcell.2020.598520

Gomez-Salazar, M., Gonzalez-Galofre, Z. N., Casamitjana, J., Crisan, M., James, A. W. and Péault, B. (2020). Five decades later, are mesenchymal stem cells still relevant? *Front. Bioengineer. Biotechnol.* **8**, 148. doi:10.3389/fbioe.2020.00148

Guo, Y., Yu, Y., Hu, S., Chen, Y. and Shen, Z. (2020). The therapeutic potential of mesenchymal stem cells for cardiovascular diseases. *Cell Death Dis.* **11**, 349. doi:10.1038/s41419-020-2542-9

Hatzistergos, K. E., Quevedo, H., Oskouei, B. N., Hu, Q., Feigenbaum, G. S., Margitich, I. S., Mazhari, R., Boyle, A. J., Zambrano, J. P., Rodriguez, J. E. et al. (2010). Bone marrow mesenchymal stem cells stimulate cardiac stem cell proliferation and differentiation. *Circ. Res.* **107**, 913-922. doi:10.1161/CIRCRESAHA.110.222703

Higuchi, T., Nekolla, S. G., Jankaukas, A., Weber, A. W., Huisman, M. C., Reder, S., Ziegler, S. I., Schwaiger, M. and Bengel, F. M. (2007). Characterization of normal and infarcted rat myocardium using a combination of small-animal PET and clinical MRI. *J. Nuclear Med.* **48**, 288-294.

Honczarenko, M., Le, Y., Swierkowski, M., Ghiran, I., Glodek, A. M. and Silberstein, L. E. (2006). Human bone marrow stromal cells express a distinct set of biologically functional chemokine receptors. *Stem Cells (Dayton, Ohio)* **24**, 1030-1041. doi:10.1634/stemcells.2005-0319

Hong, H. S. and Son, Y. (2014). Substance-p-mobilised mesenchymal stem cells accelerate skin wound healing. *Tissue Eng. Regener. Med.* **11**, 483-491. doi:10.1007/s13770-014-0062-3

Iwanaga, Y., Aoyama, T., Kihara, Y., Onozawa, Y., Yoneda, T. and Sasayama, S. (2002). Excessive activation of matrix metalloproteinases coincides with left ventricular remodeling during transition from hypertrophy to heart failure in hypertensive rats. *J. Am. Coll. Cardiol.* **39**, 1384-1391. doi:10.1016/S0735-1097(02)01756-4

Jørgensen, A. S., Daugvilaite, V., De Filippo, K., Berg, C., Mavri, M., Benned-Jensen, T., Juzenaite, G., Hjortø, G., Rankin, S., Våbenø, J. et al. (2021). Biased action of the CXCR4-targeting drug plerixafor is essential for its superior hematopoietic stem cell mobilisation. *Commun. Biol.* **4**, 1-12. doi:10.1038/s42003-021-02070-9

Karantalis, V. and Hare, J. M. (2015). Use of mesenchymal stem cells for therapy of cardiac disease. *Circ. Res.* **116**, 1413-1430. doi:10.1161/CIRCRESAHA.116.303614

Kinnaird, T., Stabile, E., Burnett, M. S., Lee, C. W., Barr, S., Fuchs, S. and Epstein, S. E. (2004). Marrow-derived stromal cells express genes encoding a broad spectrum of arteriogenic cytokines and promote in vitro and in vivo arteriogenesis through paracrine mechanisms. *Circ. Res.* **94**, 678-685. doi:10.1161/01.RES.0000118601.37875.AC

Kinugawa, K., Takahashi, T., Kohmoto, O., Yao, A., Aoyagi, T., Momomura, S., Hirata, Y. and Serizawa, T. (1994). Nitric oxide-mediated effects of interleukin-6 on [Ca2+]i and cell contraction in cultured chick ventricular myocytes. *Circ. Res.* **75**, 285-295. doi:10.1161/01.RES.75.2.285

Kucia, M., Dawn, B., Hunt, G., Guo, Y., Wysoczynski, M., Majka, M., Ratajczak, J., Rezzoug, F., Ildstad, S. T., Bolli, R. et al. (2004). Cells expressing early cardiac markers reside in the bone marrow and are mobilised into the peripheral blood after myocardial infarction. *Circ. Res.* **95**, 1191-1199. doi:10.1161/01.RES.0000150856.47324.5b

Maacha, S., Sidahmed, H., Jacob, S., Gentilcore, G., Calzone, R., Grivel, J.-C. and Cugno, C. (2020). Paracrine mechanisms of mesenchymal stromal cells in angiogenesis. *Stem Cells Int.* **2020**, 4356359. doi:10.1155/2020/4356359

Mann, D. L. (2015). Innate immunity and the failing heart. *Circ. Res.* **116**, 1254-1268. doi:10.1161/CIRCRESAHA.116.302317

Massa, M., Rosti, V., Ferrario, M., Campanelli, R., Ramajoli, I., Rosso, R., De Ferrari, G. M., Ferlini, M., Goffredo, L., Bertoletti, A. et al. (2005). Increased circulating hematopoietic and endothelial progenitor cells in the early phase of acute myocardial infarction. *Blood* **105**, 199-206. doi:10.1182/blood-2004-05-1831

Meeson, R., Sanghani-Keri, A., Coathup, M. and Blunn, G. (2019). VEGF with AMD3100 endogenously mobilises mesenchymal stem cells and improves fracture healing. *J. Orthopaedic Res.* **37**, 1294-1302. doi:10.1002/jor.24164

Odeh, M. (1993). Tumor necrosis factor-α as a myocardial depressant substance. *Int. J. Cardiol.* **42**, 231-238. doi:10.1016/0167-5273(93)90053-J

Ong, S.-B., Hernández-Reséndiz, S., Crespo-Avilan, G. E., Mukhametshina, R. T., Kwek, X.-Y., Cabrera-Fuentes, H. A. and Hausenloy, D. J. (2018). Inflammation following acute myocardial infarction: Multiple players, dynamic roles, and novel therapeutic opportunities. *Pharmacol. Ther.* **186**, 73-87. doi:10.1016/j.pharmthera.2018.01.001

Pathan, N., Franklin, J. L., Eleftherohorinou, H., Wright, V. J., Hemingway, C. A., Waddell, S. J., Griffiths, M., Dennis, J. L., Relman, D. A., Harding, S. E. et al. (2011). Myocardial depressant effects of interleukin 6 in meningococcal sepsis are regulated by p38 mitogen-activated protein kinase. *Crit. Care Med.* **39**, 1692-1711. doi:10.1097/CCM.0b013e3182186d27

Pitchford, S. C., Furze, R. C., Jones, C. P., Wengner, A. M. and Rankin, S. M. (2009). Differential mobilisation of subsets of progenitor cells from the bone marrow. *Cell Stem Cell* **4**, 62-72. doi:10.1016/j.stem.2008.10.017

Pittenger, M. F. and Martin, B. J. (2004). Mesenchymal stem cells and their potential as cardiac therapeutics. *Circ. Res.* **95**, 9-20. doi:10.1161/01.RES.0000135902.99383.6f

Ponikowski, P., Voors, A. A., Anker, S. D., Bueno, H., Cleland, J. G. F., Coats, A. J. S., Falk, V., González-Juanatey, J. R., Harjola, V.-P., Jankowska, E. A. et al. (2016). 2016 ESC Guidelines for the diagnosis and treatment of acute and chronic heart failure: The Task Force for the diagnosis and treatment of acute and chronic heart failure of the European Society of Cardiology (ESC)Developed with the special contribution of the Heart Failure Association (HFA) of the ESC. *Eur. Heart J.* **37**, 2129-2200. doi:10.1093/eurheartj/ehw128

Pouleur, A.-C., Anker, S., Brito, D., Brosteanu, O., Hasenclever, D., Casadei, B., Edelmann, F., Filippatos, G., Gruson, D., Ikonomidis, I. et al. (2018). Rationale and design of a multicentre, randomized, placebo-controlled trial of mirabegron, a Beta3-adrenergic receptor agonist on left ventricular mass and diastolic function in patients with structural heart disease Beta3-left ventricular hypertrophy (Beta3-LVH). *ESC Heart Failure* **5**, 830-841. doi:10.1002/ehf2.12306

Prabhu, S. D. and Frangogiannis, N. G. (2016). The biological basis for cardiac repair after myocardial infarction: from inflammation to fibrosis. *Circ. Res.* **119**, 91-112. doi:10.1161/CIRCRESAHA.116.303577

Rathi, S. S., Xu, Y.-J. and Dhalla, N. S. (2002). Mechanism of cardioprotective action of TNF-α in the isolated rat heart. *Exp. Clin. Cardiol.* **7**, 146-150.

Razeghian-Jahromi, I., Matta, A. G., Canitrot, R., Zibaeenezhad, M. J., Razmkhah, M., Safari, A., Nader, V. and Roncalli, J. (2021). Surfing the clinical trials of mesenchymal stem cell therapy in ischemic cardiomyopathy. *Stem Cell Res. Ther.* **12**, 361. doi:10.1186/s13287-021-02443-1

Redpath, A. N., François, M., Wong, S.-P., Bonnet, D. and Rankin, S. M. (2017). Two distinct CXCR4 antagonists mobilise progenitor cells in mice by different mechanisms. *Blood Adv.* **1**, 1934-1943. doi:10.1182/bloodadvances.2017006064

Ripa, R. S., Wang, Y., Jørgensen, E., Johnsen, H. E., Grande, P. and Kastrup, J. (2005). Safety of bone marrow stem cell mobilisation induced by granulocyte-colony stimulating factor: 30 days' blinded clinical results from the stem cells in myocardial infarction (STEMMI) trial. *Heart Drug* **5**, 177-182. doi:10.1159/000089596

Ripa, R. S., Jørgensen, E., Wang, Y., Thune, J. J., Nilsson, J. C., Søndergaard, L., Johnsen, H. E., Køber, L., Grande, P. and Kastrup, J. (2006). Stem cell mobilisation induced by subcutaneous granulocyte-colony stimulating factor to improve cardiac regeneration after acute ST-elevation myocardial infarction. *Circulation* **113**, 1983-1992. doi:10.1161/CIRCULATIONAHA.105.610469

Rombouts, W. J. C. and Ploemacher, R. E. (2003). Primary murine MSC show highly efficient homing to the bone marrow but lose homing ability following culture. *Leukemia* **17**, 160-170. doi:10.1038/sj.leu.2402763

Saini, H. K., Xu, Y.-J., Zhang, M., Liu, P. P., Kirshenbaum, L. A. and Dhalla, N. S. (2005). Role of tumour necrosis factor-alpha and other cytokines in ischemia-reperfusion-induced injury in the heart. *Exp. Clin. Cardiol.* **10**, 213-222.

Shintani, S., Murohara, T., Ikeda, H., Ueno, T., Honma, T., Katoh, A., Sasaki, K., Shimada, T., Oike, Y. and Imaizumi, T. (2001). Mobilisation of endothelial progenitor cells in patients with acute myocardial infarction. *Circulation* **103**, 2776-2779. doi:10.1161/hc2301.092122

Thielmann, M., Dörge, H., Martin, C., Belosjorow, S., Schwanke, U., van de Sand, A., Konietzka, I., Büchert, A., Krüger, A., Schulz, R. et al. (2002). Myocardial dysfunction with coronary microembolization. *Circ. Res.* **90**, 807-813. doi:10.1161/01.RES.0000014451.75415.36

Tompkins, B. A., Balkan, W., Winkler, J., Gyöngyösi, M., Goliasch, G., Fernández-Avilés, F. and Hare, J. M. (2018). Preclinical studies of stem cell therapy for heart disease. *Circ. Res.* **122**, 1006-1020. doi:10.1161/CIRCRESAHA.117.312486

Trounson, A. and McDonald, C. (2015). Stem cell therapies in clinical trials: progress and challenges. *Cell Stem Cell* **17**, 11-22. doi:10.1016/j.stem.2015.06.007

Tsutamoto, T., Hisanaga, T., Wada, A., Maeda, K., Ohnishi, M., Fukai, D., Mabuchi, N., Sawaki, M. and Kinoshita, M. (1998). Interleukin-6 spillover in the peripheral circulation increases with the severity of heart failure, and the high plasma level of interleukin-6 is an important prognostic predictor in patients with congestive heart failure. *J. Am. Coll. Cardiol.* **31**, 391-398. doi:10.1016/S0735-1097(97)00494-4

Wang, J., Tannous, B. A., Poznansky, M. C. and Chen, H. (2020). CXCR4 antagonist AMD3100 (plerixafor): from an impurity to a therapeutic agent. *Pharmacol. Res.* **159**, 105010. doi:10.1016/j.phrs.2020.105010

Warren, K., Burden, H. and Abrams, P. (2016). Mirabegron in overactive bladder patients: efficacy review and update on drug safety. *Ther. Adv. Drug Saf.* **7**, 204-216. doi:10.1177/2042098616659412

Wojakowski, W., Tendera, M., Michałowska, A., Majka, M., Kucia, M., Maślankiewicz, K., Wyderka, R., Ochała, A. and Ratajczak, M. Z. (2004). Mobilisation of CD34/CXCR4+, CD34/CD117+, c-met+ stem cells, and mononuclear cells expressing early cardiac, muscle, and endothelial markers into peripheral blood in patients with acute myocardial infarction. *Circulation* **110**, 3213-3220. doi:10.1161/01.CIR.0000147609.39780.02

Xu, H., Zhu, Z., Huang, Y. and Ildstad, S. T. (2011). The CXCR4 antagonist AMD 3100 induces rapid mobilisation of facilitating cells and hematopoietic stem cells in mice. *Blood* **118**, 4694. doi:10.1182/blood.V118.21.4694.4694

Zile, M. R., Baicu CF, Ikonomidis, S., Stroud, J., Nietert, R. E., Bradshaw, P. J., Slater, A. D., Palmer, R., Van Buren, B. M., Meyer, P. et al. (2015). Myocardial stiffness in patients with heart failure and a preserved ejection fraction. *Circulation* **131**, 1247-1259. doi:10.1161/CIRCULATIONAHA.114.013215

Zohlnhöfer, D. (2008). G-CSF for left ventricular recovery after myocardial infarction: is it time to face reality? *Cardiovasc. Drugs Ther.* **22**, 343-345. doi:10.1007/s10557-008-6114-y
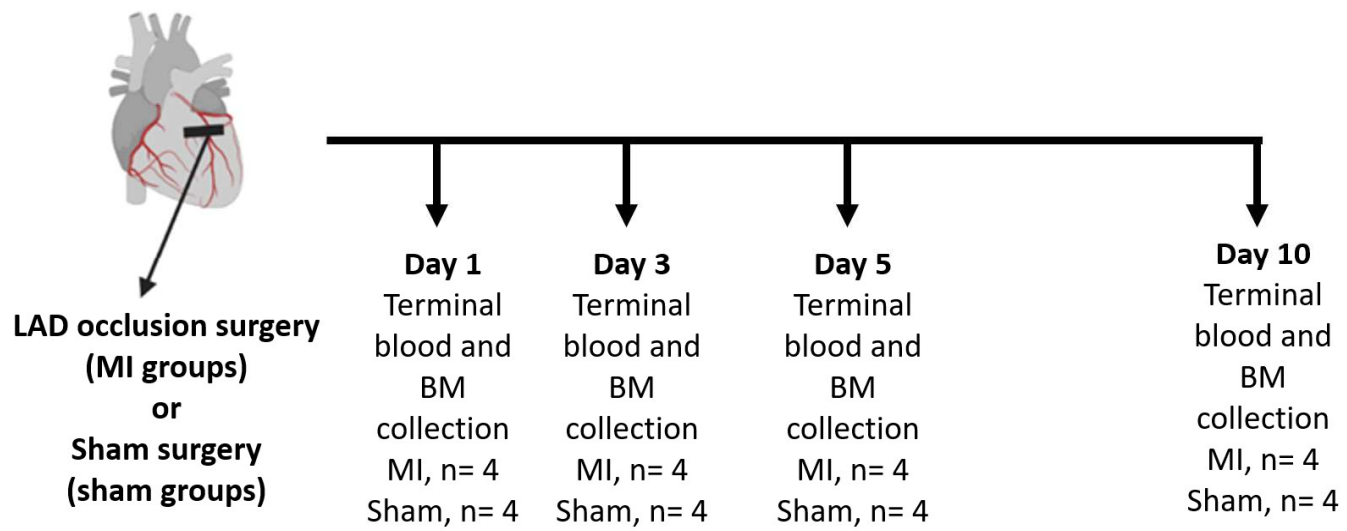
Fig. S1. Schematic representation of the experimental design for the post MI stem cell mobilisation study. A total of 32 animals were used for these experiments.
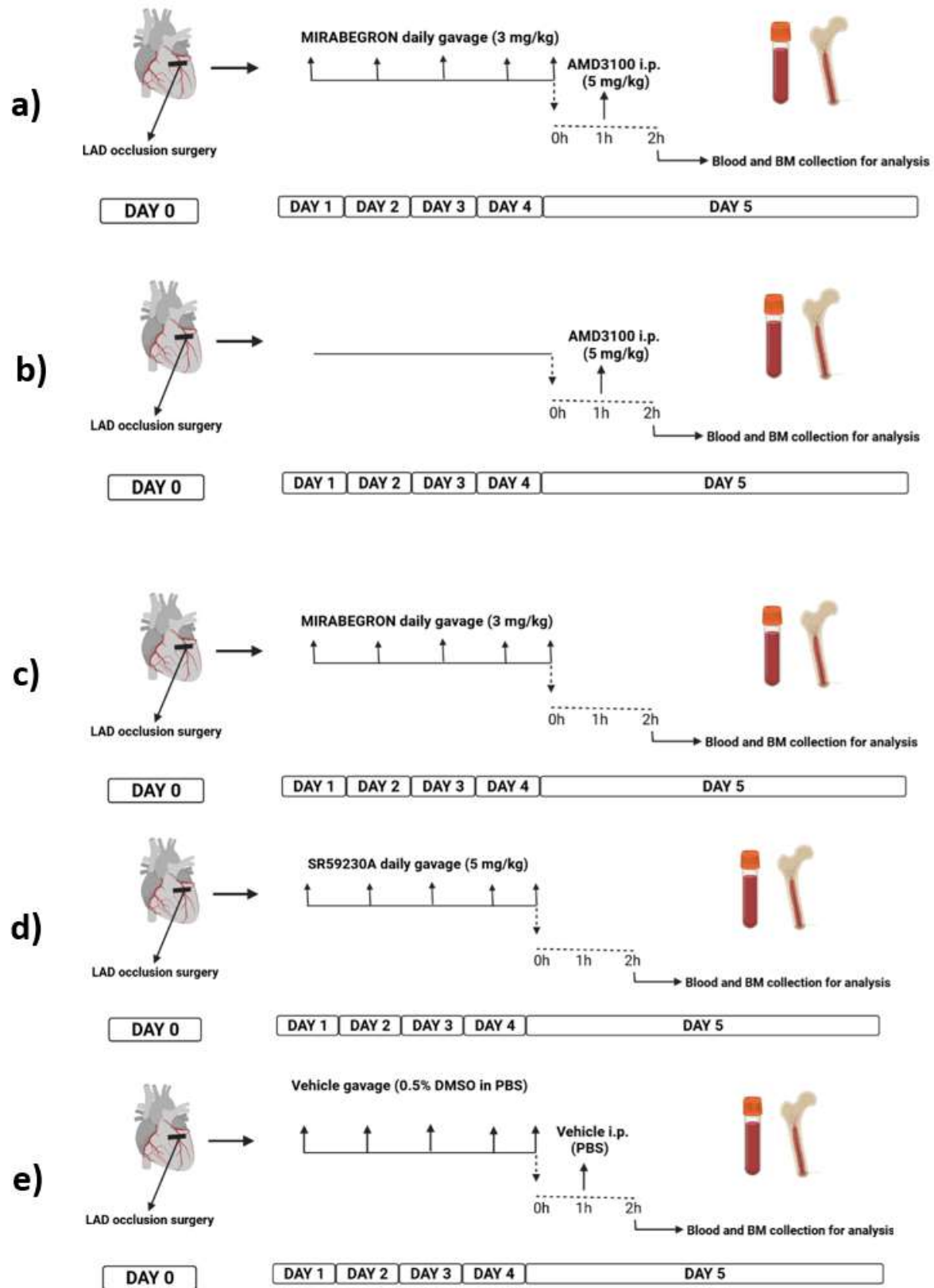
Fig. S2. Schematic representation of the drug administration regimens following MI surgery for the study of pharmacological modulation of stem cell mobilisation. A) Mirabegron+AMD3100 (MA) drug administration. B) AMD3100 only (A) drug administration. C) Mirabegron only (M) drug administration. D) SR59230A (SR) drug administration. E) Vehicle (V) group drug administration. Created with Biorender.com
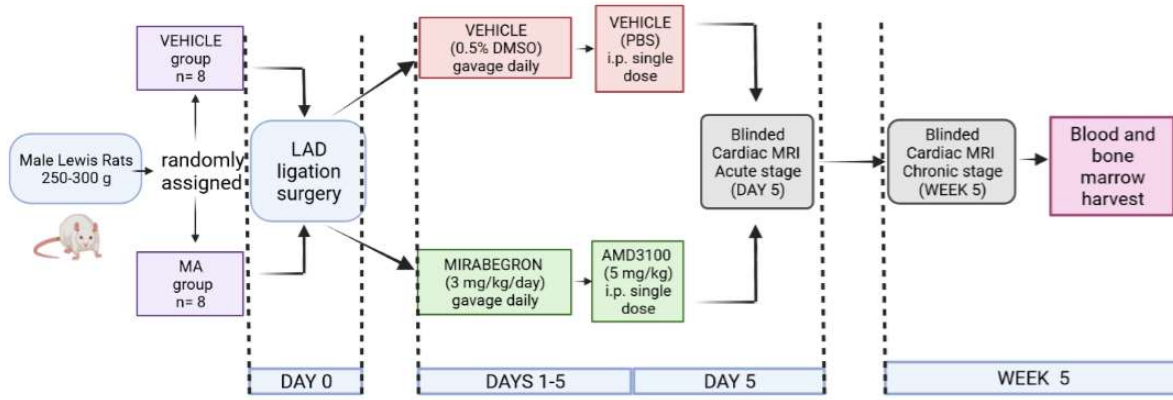
Fig. S3. Study design for assessment of the effect of mirabegron+AMD3100 treatment on cardiac function after MI. One rat from each group died within 24h of surgery, reducing the n number from 8 to 7 for each group. One rat from the vehicle group was excluded due to lack of significant infarct (<10%), reducing the vehicle group to n= 6. (Created with BioRender.com)
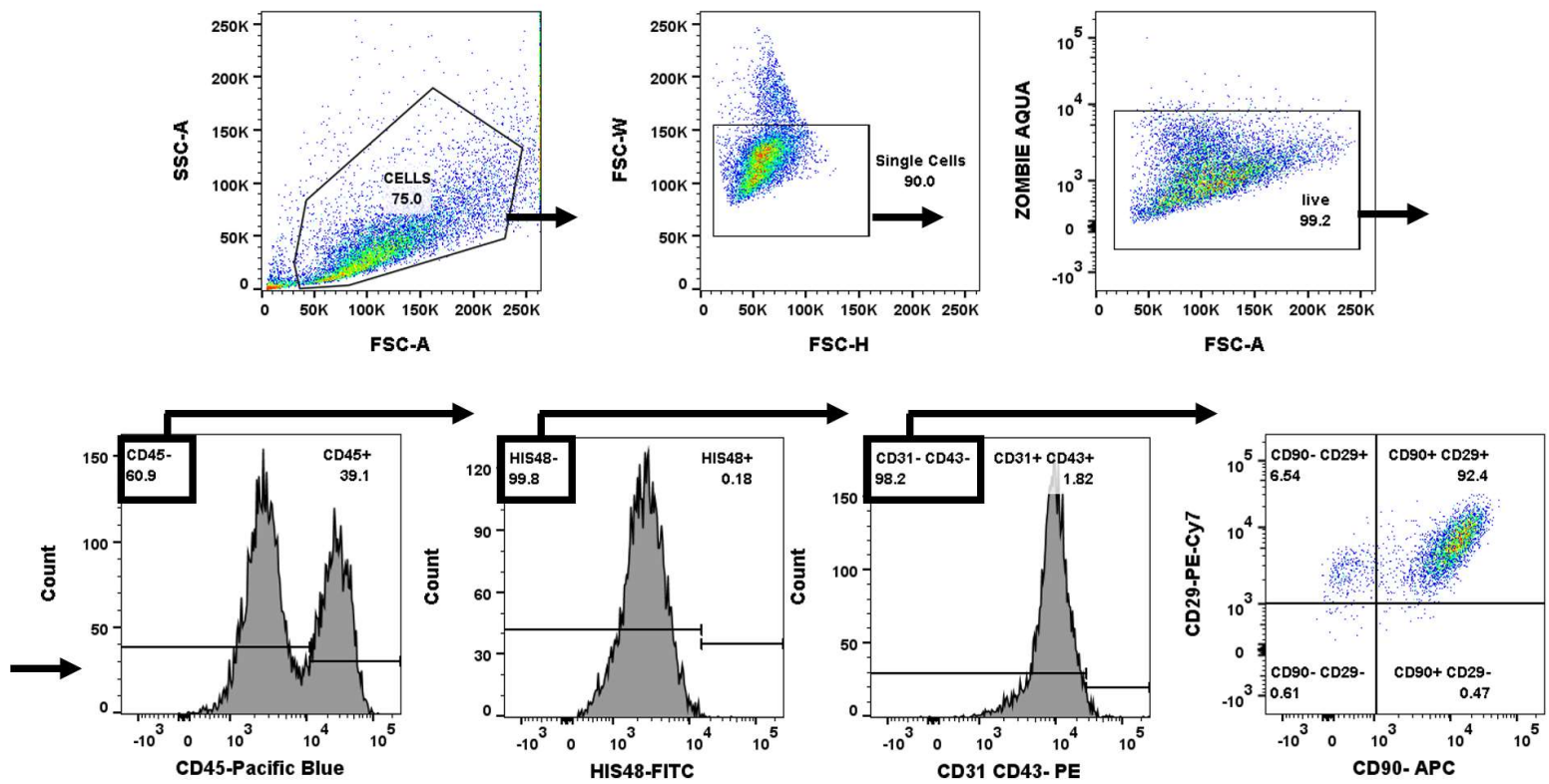

Fig. S4. Gating strategy for the flow cytometry analysis of BM and blood derived culture expanded CFU-Fs. From left to right, top to bottom: first we gated into whole cells to exclude debris (FSC-A, SSC-A), then the single cells were gated into (FSC-H, FSC-W), followed by the live cells (Zombie Aqua™ negative). These were then gated into the CD45-negative fraction, to exclude haematopoietic cells, followed by exclusion of the HIS48+ and CD31+ CD43+ to remove any granulocytes, endothelial cells, and monocytes. Finally, we looked at the CD90 and CD29 expression to determine the rat MSC cell surface marker expression.
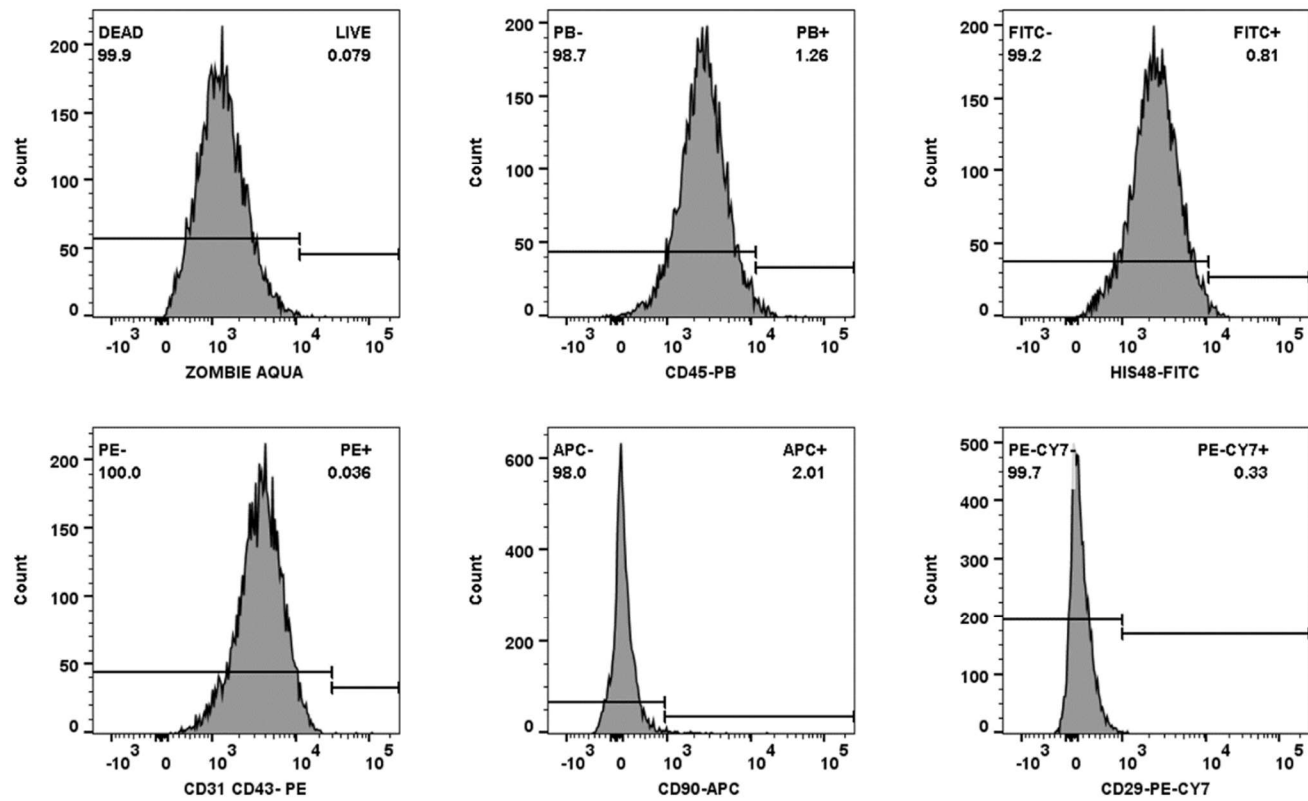
Fig. S5. Fluorescence minus one (FMO) controls for the flow cytometry analysis. Here we show the gates we used in our analysis, based on the FMO controls, which included all but one marker to ensure that the appropriate negative population is being gated out. From left to right, top to bottom we show the gates for Zombie Aqua (live/dead), Pacific Blue (CD45), FITC (HIS48), PE (CD31, CD43), APC (CD90), PE-Cy7 (CD29).
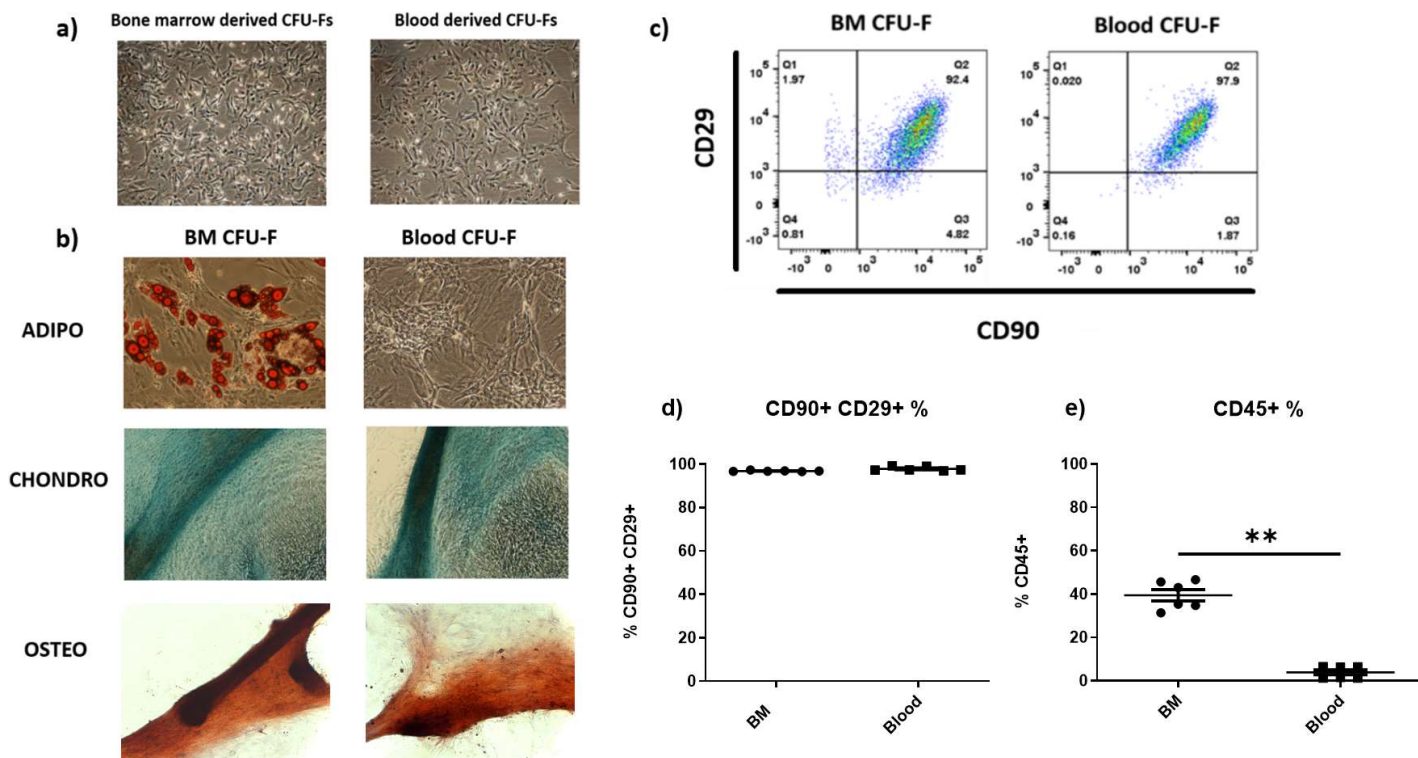
Fig. S6. MSCs characterisation. A) Blood and BM derived CFU-Fs were fibroblast like and plastic adherent in culture. Brightfield image, 10X. B) Blood and BM derived CFU-Fs were culture expanded (P2-P8) and induced to differentiate into adipo-, chondro- and osteocytes. Culture expanded CFU-Fs from the BM (vehicle and SR groups), but not from the blood and BM (MA, M, A groups), differentiated into adipocytes (fat droplets stained red by Oil Red-O), both BM and blood derived CFU-Fs differentiated into chondrocytes (glycosaminoglycans stained blue by Alcian Blue) and osteocytes (calcium deposits stained in brick red by Alizarin Red S). C) Blood and BM culture expanded (P2-P8) CFU-Fs were double positive for CD90 and CD29 (gated on live, single, CD45-, CD43-, CD31- , His48- cells). D) Percentages of double positive CD90+ CD29+ BM and blood derived CFU-Fs (gated on live, single, CD45-, CD43-, CD31- , His48) (Unpaired t test, p= 0.0562, n=6) E) Percentage of CD45+ cells in BM and blood derived CFU-Fs (gated on live, single cells) (Mann-Whitney test, p= 0.0022, n=6)
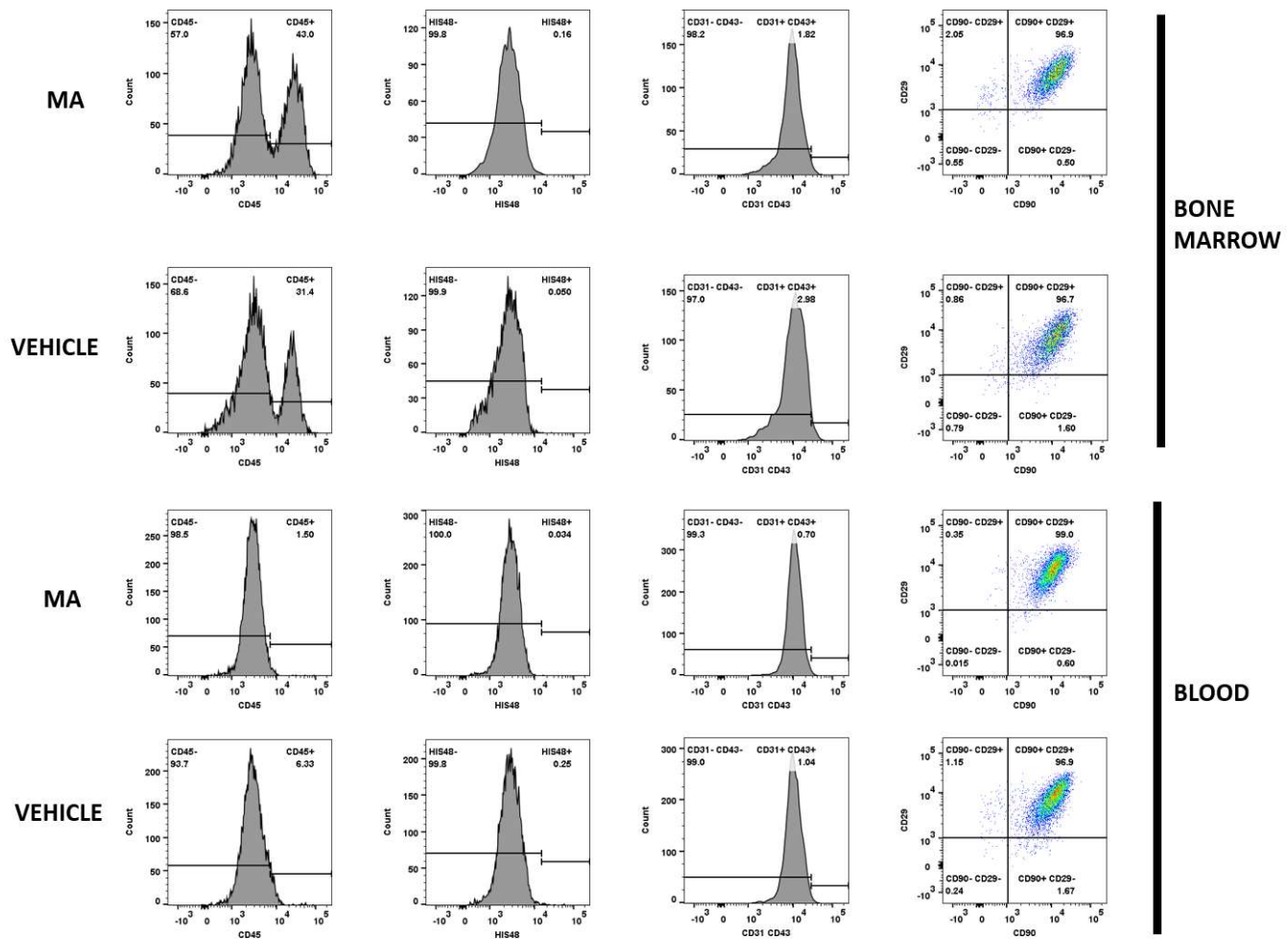
Fig. S7. Representative histograms and scatter plots of the flow cytometry data. Here we have shown representations of the flow cytometry data for the BM and blood derived culture expanded CFU-Fs (MSCs) from both groups: vehicle and MA. The gating is shown in the Supplementary Methods.
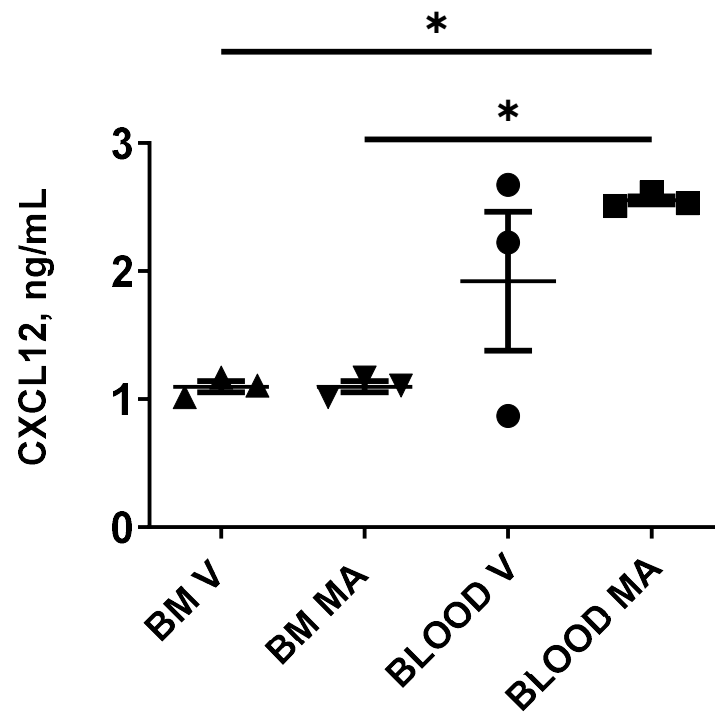
Fig. S8. CXCL12 levels in conditioned medium (CM) from blood and BM derived MSCs. This graph shows the CXCL12 concentration (ng/mL) in the CMs from culture expanded blood and BM MSCs from the vehicle and MA groups. The data were obtained using the sandwich ELISA method. (Ordinary One-Way ANOVA, Tukey post-test, * $p < 0.05$, n= 3)

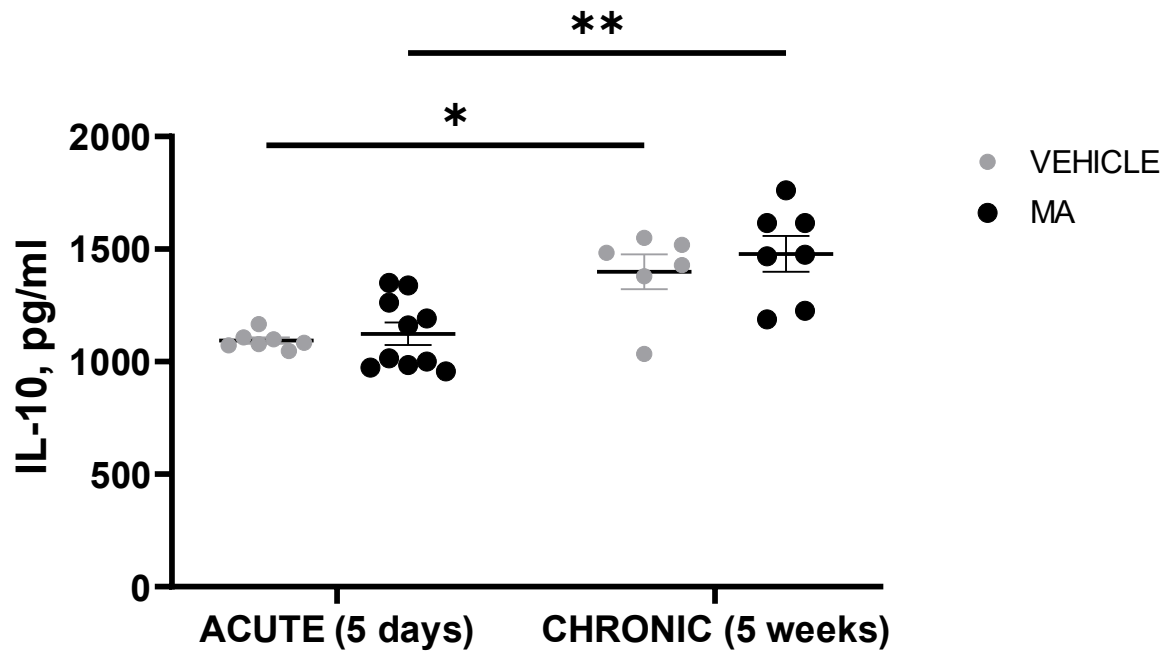**Fig. S9. IL-10 levels in the plasma of the vehicle and MA treated groups at 5 weeks post MI.** The IL-10 concentration is given as pg/mL, Two Way ANOVA, Sidak's multiple comparisons test, * p< 0.05, ** p< 0.01, vehicle n= 6, MA n= 7
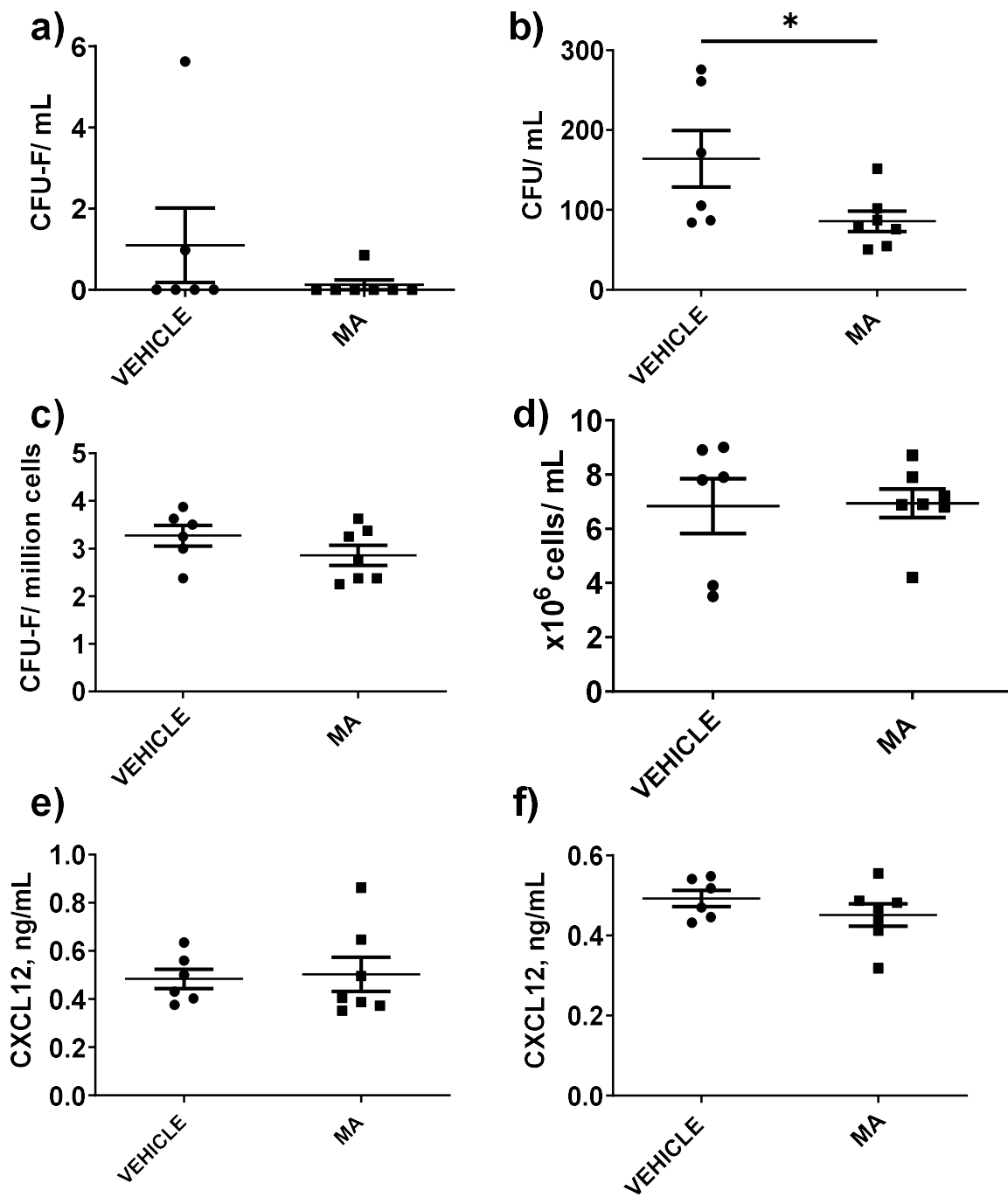
Fig. S10. Stem/progenitor mobilisation dynamics at 5 weeks post MI. This graph summarises the stem/progenitor mobilisation dynamics in the vehicle (n= 6) and MA group (n= 7). A) Circulating MSPCs are represented as CFU-F/mL (Mann-Whitney test, p= 0.3147). B) Circulating HSPCs are shown as CFU/mL (Unpaired t-test, p= 0.0494). C) BM MSPC numbers are shown as CFU-F/ million cells (Unpaired t-test, p=0.2003). D) Circulating total nucleated cells are shown as million cells/mL (Unpaired t-test, p=0.9229). Plasma (E) and BM (F) CXCL12 are shown as ng/mL, (Mann-Whitney test, p= 0.7308 and p= 0.4452, respectively)

Fig. S11. Example images of tube formation assay and wound healing assay. (A) Example images from the tube formation assay are given for each grou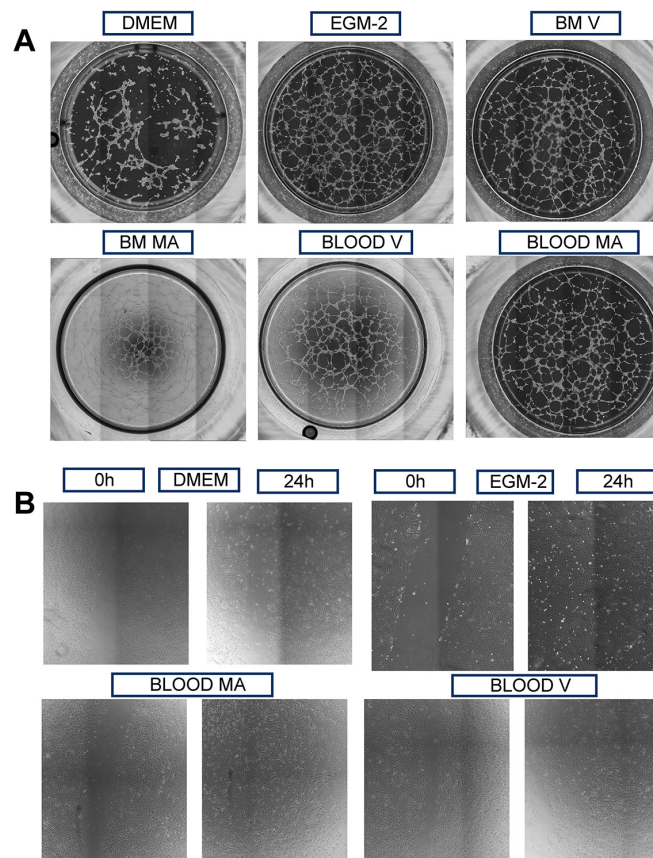p: HUVECs treated with DMEM (negative control), EGM-2 (positive control), conditioned medium from blood-derived rat MSCs (rMSCs) from the MA group (BLOOD MA), conditioned medium from blood-derived rMSCs from the Vehicle group (BLOOD V), conditioned medium from bone marrow-derived rMSCs from the MA group (BM MA), conditioned medium from BM-derived rMSCs from the Vehicle group (BM V). (B) Example images from the wound healing assay are given for HUVECs treated with DMEM (negative control), EGM-2 (positive control), conditioned medium from blood-derived rMSCs from the MA group (BLOOD MA) and conditioned medium from blood-derived rMSCs from the Vehicle group (BLOOD V). The time after producing the scratch ('wound') is indicated as 0 h (immediately after) and 24 h (24 h after).

Table S1. List of fluorophore-conjugated antibodies used in our analysis of culture expanded bone marrow and blood derived CFU-F.

Fluorophore	Rat Antigen	Clone	Manufacturer
Pacific Blue™	CD45	OX-1	Biolegend
PE	CD43	W313	Biolegend
PE	CD31	TLD-3A12	BD Biosciences
APC	CD90	OX-7	Biolegend
PE-Cy7	CD29	HMb1-1	Biolegend
FITC	Granulocyte marker	HIS48	Invitrogen
Zombie Aqua	Dead cells	-	Biolegend
n/a	CD32, Fc block	D34-385	BD Biosciences

Supplementary Materials and Methods

Animal studies: experimental design and drug administration

For the study investigating the natural stem cell mobilisation post MI, Lewis rats in the MI group underwent left anterior descending artery (LAD) ligation surgery, and the animals in the sham group underwent a sham surgery, which did not include tying of the suture around the vessel. For each timepoint we assessed 4 animals in each group (MI and sham), and we had a total of four timepoints: day 1, 3, 5, and 10 (Fig. S1). The rats were culled at each of these endpoints for collection of peripheral blood (PB) by cardiac puncture and hind legs for bone marrow (BM) extraction.

For the drug selection study, all rats underwent MI inducing surgery and were randomly assigned to five groups: vehicle (n= 8), mirabegron only (M, n= 8), AMD3100 only (A, n= 8), mirabegron+AMD3100 (MA, n= 12), and SR59230A (SR, n= 8). Only two surgeries a day could be performed, meaning that the experiments were spaced

out in time. Thus, we decided to include additional animals in the MA group to maximise the probability of them being more evenly distributed throughout the study and to also account for potential loss of animals, as this was the main group of interest. The surgeon was blinded to the group assignment. To the MA group, mirabegron (YM178, ApexBio) was given at 3 mg/kg/day using the gavage method for five days post MI starting at 24h after surgery, and after 5 days AMD3100 (AMD3100 octahydrochloride hydrate, Sigma) was administered, one hour after the last dose of mirabegron, at 5 mg/kg using the intraperitoneal injection method (Fig. S2a). The A group received only the single dose of AMD3100 (5 mg/kg) (Fig. S2b), the M group received only the daily gavage of mirabegron (3 mg/kg) (Fig. S2c), and the SR group received daily gavage of the β_3AR antagonist SR59230A (SR 59230A hydrochloride, Tocris) (5 mg/kg) for the first five days after MI (Fig. S2d). The vehicle group received 0.5% dimethylsulfoxide (DMSO) for 5 days (gavage) and a single dose (i.p.) of phosphate buffered saline (PBS) on the last day (Fig. S2e). The BM and PB samples were collected 1h after the final drug injection on day 5 for stem/progenitor cell enumeration and cytokine and chemokine level analysis. As the scar sizes were estimated using Masson's trichrome, all animals that had a scar size of less than 10% were excluded: vehicle (n= 1), AMD3100 only (n= 2), mirabegron+AMD3100 (MA, n= 2) and SR59230A (n= 2), which lead to the final n numbers of: vehicle (n= 7), mirabegron only (M, n= 8), AMD3100 only (A, n= 6), mirabegron+AMD3100 (MA, n= 10) and SR59230A (SR, n= 6).

The final animal study looked at the effect of mirabegron+ AMD3100 (MA) on cardiac function at 5 weeks after MI surgery. The experimental design is summarised in Figure S3 below. The drug administration regimens for the MA and the vehicle groups were the same as in the drug selection study described above (Fig. 2a, e). Briefly, MI inducing surgery was performed on Lewis rats, which were randomly assigned to two groups: vehicle and MA. The animal surgeon was blinded to group assignment at the time of surgery. Each group then received the corresponding treatment and at day 5 after the last drug administration they underwent the first cardiac MRI (acute stage), which was then followed with the second cardiac MRI 5 weeks later (chronic stage). The animals were culled at the 5-week timepoint following the second MRI scan and the PB, BM and hearts were collected for analysis.

Differentiation assays

Differentiation assays were performed in 24-well plates with cells seeded at $2x10^5$ per well for the adipogenesis and osteogenesis and $4x10^5$ for the chondrogenesis and expanded until confluent in DMEM+GlutaMax™ supplemented with 20% FBS (D20) before changing to the defined differentiation induction media. Media changes were performed every 3-4 days. The adipogenic differentiation medium was α-MEM+ GlutaMax™, supplemented with 10% FBS, 1 uM dexamethasone, 0.2 mM indomethacin, 10 μg/mL insulin, 0.5 mM 3-isobutyl-1-methylxanthine (IBMX), and 3.5 g/L glucose. Fat droplets were stained in red by using Oil-red-O as described previously [1]. The osteogenic differentiation medium was α-MEM+ GlutaMax™, supplemented with 10% FBS, 0.01 μM dexamethasone, 10 mM beta-glycerophosphate, 0.2 mM ascorbic acid-2- phosphate, 3.5 g/L glucose. Calcium deposits were stained in brick red by Alizarin Red S as described previously [1]. The chondrogenic differentiation medium was DMEM+GlutaMax™, supplemented with 10% FBS, 0.1 μM dexamethasone, 50 μg/mL ascorbic acid-2- phosphate, 40 μg/mL L-proline, 1x ITS+3 supplement, 10 ng/ml TGF-beta 3, 1% sodium pyruvate, 4.5 g/L glucose. Glycosaminoglycans were stained in blue by using Alcian Blue as described previously [1].

Flow cytometry analysis

Flow cytometry analysis was done on cultured plastic adherent BM and blood CFU-F derived cells to assess their expression of the cell surface markers CD45, HIS48, CD31, CD43, CD90 and CD29, which were selected based on previous work that shows CD90+ CD29+ CD45- CD31- HIS48- CD43- to be a rat MSC marker panel [2-5]. The list of antibodies we used is included in Table S1 below. All steps were done on ice and flow buffer (2% FBS in PBS) was used for all staining except the live/dead stain Zombie Aqua™, which was done in PBS only. Cells were pelleted in a 96-well plate for the staining procedure. Unspecific binding was prevented using Fc block (1:200) prior to staining. After this, samples were stained with Zombie Aqua™ (1:200) for 10 min to separate dead cells from the analysis. Finally, the fluorophore-conjugated antibodies were added to the cells and incubated in the dark for 30 min. The cells were washed and resuspended for analysis on the LSR Fortessa II. We used the following controls: compensation (single stains) and 'fluorescence minus one' (FMO) controls. Compensation was done manually using the single stained cells. The gating strategy is summarised in Fig. S4 and the FMO controls are shown in Fig. S5. We used the FMO controls to set the negative gates for the analysis.

Sandwich ELISAs for CXCL12, TNF-alpha, IL-6, and IL-10

The protein concentrations of the chemokine CXCL12 and the cytokines IL-6, TNF-alpha and IL-10 were analysed using the sandwich ELISA method. All antibodies were acquired from Peprotech. Briefly, the plates were coated with the capture antibodies overnight and were washed using washing solution (WS, 0.5% Tween in PBS) prior to blocking with blocking solution (BS,10% FBS in PBS) for an hour. The plates were then washed with WS, and the plasma or BM supernatant samples were added and incubated overnight. Following another wash step, the primary antibodies conjugated

to biotin were added for an hour. After this, plates were washed and the streptavidin-HRP was added for 30 min. Plates were washed again and the TMB substrate was added until full colour development, after which the reaction was stopped with sulphuric acid (1 mol/L). Results were read in a plate reader at 450 nm.

Histology

Following the sacrifice of the animal, the heart was excised, washed in heparinised PBS, and fixed in 4% Histofix overnight. Following fixation, the hearts were stored in 70% ethanol. The hearts were embedded in wax, 4 µm sections were obtained and Masson's trichrome staining was performed. Immunofluorescent staining was performed on heart sections according to the following protocol: sections were dewaxed in neoclear for 20 min, then rehydrated in increasing percentages of ethanol - 100% (10 min), 95% (5 min), 70% (5 min), 30% (5 min), distilled water (5 min). Following this, antigen retrieval was done by boiling the slides in citrate buffer (pH= 6) for 20 min. The slides were then permeabilised using 0.1% Triton/PBS for 10 min and following this were rinsed in tap water for 5 min. The sections were coated with blocking solution for 1h prior to addition of the primary antibodies. These were diluted in the same blocking solution (10% normal goat serum in 0.1% BSA in PBS). Antibodies were allowed to incubate overnight at 4°C. For the isolectin-B4 staining we used isolectin-B4 conjugated to biotin. Three 10-minute washes in PBS were performed prior to adding the secondary antibodies (streptavidin- Alexa Fluor™ 555) were added and incubated overnight in the same way. Finally, the sections were stained with DAPI and mounted using ProLong™ Gold Antifade Reagent. Images were acquired using AxioObserver Z1 and the data was analysed using ImageJ, with a customised macro for blood vessel density quantification. For the scar size and interstitial fibrosis quantification, we used the Masson's trichrome images of the 5 weeks post MI heart

sections, and a macro was written for both types of analysis. For the scar size quantification, the whole section was analysed, and for the IF, the percentage collagen was calculated against the whole tissue measured: LV and border zone regions were selected manually. For all histology, we performed blinded analysis using a total of 6 levels of the heart, spaced 250 μm.

In vitro angiogenesis assays

Human umbilical vein endothelial cells (HUVECs) were purchased from Lonza and were used between passage 1-6. For the tube formation assays, we used the Ibidi μ-Slide Angiogenesis slides as per manufacturer's instructions. The wound healing assay was performed as described previously [6]. Images were taken on a widefield microscope (AxioObserver Z1) and analysed using ImageJ. For the tube formation assay we used an Angiogenesis Analyzer macro developed for ImageJ [7].

To obtain the conditioned media (CMs), the blood and BM derived culture expanded CFU-Fs (MSCs) were allowed to become confluent in a T25 flask and were then washed with serum-free DMEM and fed serum free DMEM for 24 hours. The CMs were then aspirated and filtered through a 0.2-μm filter for use in the tube formation and wound healing assays.

Cardiac MRI

Rats were anesthetised using 5% isoflurane and maintained under inhalational anaesthesia via a nose cone (2.5% isoflurane). Vital signs and ECG were continuously monitored. All MRI scans were performed on a pre-clinical 9.4 T scanner (94/20 USR Bruker BioSpec; Bruker Biospin, Ettlingen, Germany) housed at the Biological Imaging Centre (BIC), Imperial College London equipped with a volume transmit quadrature coil combined with an actively decoupled rat heart array receiver. Data were acquired

with Paravision 6.01 (Bruker, BioSpin). For localisation of the heart, low-resolution ECG and respiratory triggered gradient echo scout scans were acquired in axial, sagittal and coronal orientations followed by pseudo two- and four-chamber gradient echo scans. Left ventricular EF, mass, ESV and EDV were quantified from a stack of ECG and respiratory-gated CINE gradient echo images in the short-axis plane (11-12 slices). The acquisition parameters for CINE measurements were: repetition time (TR)=RR interval/number of frames (~9 ms for 20 frames), TReffective=RR interval, echo time (TE)=2.2 ms, flip angle=18°, slice thickness=1.5 mm (continuous slices), acquisition matrix=190×190, field of view = (38.5×38.5) mm2, leading to a spatial in-plane resolution of (202×202) µm2, scan time: 18-20 min.

Multi slice late gadolinium enhancement (LGE) data were acquired using an inversion recovery gradient echo sequence with a single TI point and flip angle of 90°. The TI was selected to effectively null the healthy myocardium and to provide the best contrast enhancement of the area of infarction. Infarction size (acute stage) and fibrosis (chronic stage) was quantified by tracking the LGE signal for each LV axial slice using the in-built function in the open-source software Segment (version 2.2, Medviso AB, Lund, Sweden). The following acquisition parameters were used: TE = 2.4 ms, TRs = 3.85 ms, FOV = (38 ×38) mm2, matrix size = 180 × 180, spatial resolution (211×211) µm2, 1.5 mm slice thickness, 9-10 slices, scan time: 3 min /slice. All MRI data underwent blinded analysis.

Supplementary references

1. Karaoz, E., Aksoy, A., Ayhan, S., Sariboyaci, A.E., Kaymaz, F., Kasap, M., 2009. Characterization of mesenchymal stem cells from rat bone marrow: ultrastructural properties, differentiation potential and immunophenotypic markers. Histochem Cell Biol 132, 533–546. https://doi.org/10.1007/s00418-009-0629-6

2. Miyahara, Y., Nagaya, N., Kataoka, M., Yanagawa, B., Tanaka, K., Hao, H., Ishino, K., Ishida, H., Shimizu, T., Kangawa, K., Sano, S., Okano, T., Kitamura, S., Mori, H., 2006. Monolayered mesenchymal stem cells repair scarred myocardium after myocardial infarction. Nat Med 12, 459–465. https://doi.org/10.1038/nm1391

3. Lotfy, A., Salama, M., Zahran, F., Jones, E., Badawy, A., Sobh, M., 2014. Characterization of mesenchymal stem cells derived from rat bone marrow and adipose tissue: a comparative study. Int J Stem Cells 7, 135–142. https://doi.org/10.15283/ijsc.2014.7.2.135

4. Harting, M., Jimenez, F., Pati, S., Baumgartner, J., Cox, C., 2008. Immunophenotype characterization of rat mesenchymal stromal cells. Cytotherapy 10, 243–253. https://doi.org/10.1080/14653240801950000

5. Fafián-Labora, J., Fernández-Pernas, P., Fuentes, I., De Toro, J., Oreiro, N., Sangiao-Alvarellos, S., Mateos, J., Arufe, M.C., 2015. Influence of age on rat bone-marrow mesenchymal stem cells potential. Sci Rep 5, 16765. https://doi.org/10.1038/srep16765

6. Liang, C.-C., Park, A.Y., Guan, J.-L., 2007. In vitro scratch assay: a convenient and inexpensive method for analysis of cell migration in vitro. Nat Protoc 2, 329–333. https://doi.org/10.1038/nprot.2007.30

7. Carpentier, G., Berndt, S., Ferratge, S., Rasband, W., Cuendet, M., Uzan, G., Albanese, P., 2020. Angiogenesis Analyzer for ImageJ — A comparative morphometric analysis of "Endothelial Tube Formation Assay" and "Fibrin Bead Assay." Sci Rep 10, 11568. https://doi.org/10.1038/s41598-020-67289-8